DISTRIBUTIONS OF TIME-AVERAGE VELOCITIES OF DIFFUSING SLOT JETS

OF VARIOUS LENGTH-WIDTH RATIOS

by

Vujica M. Yevdjevich

January 15, 1965

CER65VMY8

DISTRIBUTIONS OF TIME-AVERAGE VELOCITIES OF DIFFUSING SLOT JETS OF VARIOUS LENGTH-WIDTH RATIOS

BY

Vujica M. Yevdjevich

ENGINEERING RESEARCH CENTER

Colorado State University

Fort Collins, Colorado

January 15, 1965

CER65VMY8

ACKNOWLEDGEMENTS

Acknowledgement is due to research assistants, and graduate students at Colorado State University. Mr. James B. Bole contributed substantially in setting-up research facilities and instrumentation as well as in taking the experimental data. Mr. Larry A. Roesner was closely related to this study in all phases of the work: experimental work, analysis of data, and presentation of results; his contribution was very valuable. Mr. Raymond L. Jeng participated effectively in the experimental work and in the data processing. Thanks are to Mrs. Arlene Reid for typing this manuscript.

TABLE OF CONTENTS

TABLE OF CONTENTS - continued

DISTRIBUTIONS OF TIME-AVERAGE VELOCITIES OF DIFFUSING SLOT JETS OF VARIOUS LENGTH-WIDTH RATIOS

by Vujica M. Yevdjevich*

1. INTRODUCTION

1.1 Statement of the problem investigated.

The diffusion of submerged jets in an environment, involving the same fluid characteristics of both the jet and the environment, has been studied extensively for two cases: (a) jets with a circular outlet orifice; and, (b) rectangular jets having an orifice with a very large length-width ratio. In the following text, these two types of jets will be called "circular jet" ** and "slot jet", respectively. In the latter case, the jet flow patterns in the central cross section through jet axis, which is perpendicular to the long side of slot orifice, approximate well at least for finite distances from the orifice, the diffusion patterns of a two-dimensional jet of infinite slot length. The slots are defined as jet outlet orifices of rectangular cross section, with long side L_o and short side B_o. The length-width ratio L_o/B_o and the orifice area $A_o = L_o B_o$ are the main geometric characteristics of rectangular slots.

Jets are usually divided into free jets and jets issuing into fluids that are not at rest. Only free submerged jets with a single composition of jet fluid and environmental fluid, are studied here. These jets are further divided into laminar flow jets and turbulent flow jets. Only turbulent flow jets are studied here.

The time-average velocity at a point in a turbulent flow is defined

---

*) Professor of Civil Engineering, Colorado State University, Fort Collins, Colorado.

**) The expressions "round jet" or "radial jet" are also often used in literature and are synonymous with "circular jet."

as the mean value of a velocity which fluctuates in time as the consequence of flow turbulence. Equations for time-average velocity distributions of diffusing jets and other diffusion equations, for the case in which there is no difference in properties of the jet fluid and the environmental fluid (such as differences in density, viscosity, miscibility, etc.), have been studied theoretically and verified experimentally. These equations refer either to circular jets, or to two-dimensional slot jets of very large length-width ratios. Equations for these two cases differ substantially, as will be shown later; however, the diffusion characteristics of the square slot jet may be considered as approximating the characteristics of the circular jet.

Information is needed for the velocity distributions and the other characteristics of slot jets for which the length-width ratio changes from unity (square jet) to a very large value (two-dimensional infinite slot jet). Experiments have been conducted at Colorado State University Engineering Research Center to investigate the problem of distribution of time-average velocity of diffusing jets when the length-width ratio of slots is finite and are reported in this paper.

The objective of the experiments conducted and of this study is not the development of a new theoretical approach to slot jet diffusion, but is rather an investigation with intent of filling the gap in knowledge of velocity distribution properties of slot jets for slots of finite and especially of small length-width ratios. The case of a slot jet with an orifice of a very large length-width ratio is assumed here to have the same characteristics for finite distances from the jet orifice as two-dimensional jet of infinite slot length. Main aspects of the problem are the shape and "carry of the jet" as the jet fluid penetrates deeper and deeper into the environment, and the entrainment of environmental fluid with the jet. This entrainment reduces any difference in fluid properties between the miscible fluids of the jet and the environment.

Diffusing jets which enter an environment of approximately the same fluid characteristics are frequently referred to as free submerged jets. The term "free" means that the boundaries of the environment are far from the jet zones being investigated. The term "submerged" primarily refers to liquid jets which enter the environment far below the liquid free surface (if any), so that the free surface has a small effect on the diffusion at least for limited distances from the jet orifice. The terms "free submerged jet" or simply "submerged jet" will be used in this text exclusively with the definition given here. The orifice is defined as the last cross section of solid boundaries before the jet enters the environmental fluid.

1.2 Mechanics of jet diffusion.

When a concentrated jet enters the environment of a fluid which is at rest, the jet turbulence and the viscous shear between the moving jet and the fluid at rest create turbulence in the contact region. The jet will thus be subjected to lateral diffusion and deceleration by the fact that the momentum of the jet will be transferred to the surrounding fluid. The environmental fluid in turn will be accelerated, causing the surrounding region of the jet to be brought into motion.

Due to turbulent fluctuation, the fluid velocity of the jet and the velocity of the entrained environmental fluid at any point in the environment outside the regions of laminar regime fluctuate with time. This time fluctuation may be characterized by the distribution of the random variable, velocity, and by the stochastic process of velocity time series at that point. The time-average velocity is considered here as the main characteristic of the velocity time series at that point. This time-average velocity as it changes from point to point determines, for the purposes of this study, the velocity distribution of a diffusing jet as it penetrates an environmental fluid. Therefore, no effort is planned here to investigate the other characteristics of the velocity time series at a point, such as the characteristics of instantaneous fluctuating velocity components u', v' and w', and their relationship in time and space. This approach is being used regardless of the fact that the turbulent velocity fluctuation at a point plays an important role in jet diffusion. The mean flow pattern of diffusing jets, in the region of jet penetration and expansion, is defined here by the distribution of the time-average velocity. The reader is referred to the most recent literature for the characteristics of turbulence in jet expansion especially with well designed experiments [55]*.

A high-velocity jet entering a fluid at rest represents an irrecoverable loss of energy, although in some cases, there may be a temporary conversion of kinetic energy into potential energy and vice versa. When a jet enters a fluid at rest, such as the fluid in a large chamber, a large reservoir or the atmosphere, the basic axiom of fluid mechanics requires that the entire kinetic energy of the jet be dissipated finally by turbulence through viscous shear, and interaction with the environmental fluid. The mechanical process of dissipation is simple; the kinetic energy continuously creates turbulence which results in viscous shear as the means of energy dissipation. If the kinetic energy of the jet is converted into potential energy of increased pressure in a confined region, the pressure differences thus created with the adjacent regions will accelerate and move the environmental fluid in bulk. This in turn represents a reconversion of potential energy to kinetic energy, with the generation of new turbulence (in turbulent flow regime) and of new viscous shear in both the turbulent and the laminar flow regime.

---

*) The numbers in brackets refer to the references at the end of this text.

It should be stressed here that (for the case of a jet diffusing in a confined region) besides the momentum transfer from the jet to the environmental fluid and its acceleration upon their contact, the conversion of a part of the kinetic energy of the jet into an increased local pressure also accelerates the environmental fluid and moves it in the direction of the pressure gradient. This is especially true for the case of confined environments like ducts, tunnels, chambers and similar installations.

1.3 Boundary conditions of the jet orifice and of the environment.

The diffusion of a submerged jet in an environment depends on the boundary conditions, both of the jet orifice and of the environment, if the environment is confined. The relationship of the jet-bearing fixed contours to the environment is of great importance. As the jet entrains the environmental fluid, these contours determine the stream lines of the entrained fluid around the jet. Some investigators have assumed or experimented with the jet orifice being the opening in a vertical wall with the jet horizontally directed, or the opening in a horizontal wall with the jet directed upwards or downwards into the environmental fluid.

The boundaries of the environment when it is confined play an important role in jet studies. At a sufficient distance from the orifice the diffusion of a jet in a duct or in a tunnel has clearly different properties than a jet which enters a practically unlimited environment such as the free atmosphere, a deep reservoir, or a deep sea. All transitions exist in practice between a duct-type environment and a very vast and practically unlimited environment.

General patterns of jet diffusion and jet deceleration as it relates to boundary conditions are as follows. The entrance of a jet through a long pipe into an unconfined environment (assuming that the jet orifice carrier and jet fluid access have the minimum space occupancy in the environment) represents a case in which a minimal obstacle exists for the entrainment of environmental fluid with a maximal effect on the deceleration of jet. With an increase of space occupancy by fixed boundaries around the jet orifice and with a decrease of dimensions of the environment, both the volume of entrained fluid and the rate of jet deceleration will be somewhat decreased. A jet diffusing in a ducted environment with small dimensions tends to preserve higher velocities than in the case of an unconfined environment, especially along the jet-axis for that portion of the duct before the effects of friction by the walls prevail. The environmental dissipation of jet energy is supplemented, in a duct, by energy loss due to friction along the duct walls.

Distributions of time-average velocity in a ducted environment or in a narrow chamber may be approximately determined by applying the principle of "mirror reflection" of velocity distributions in an unconfined environment to the duct walls. The time-average velocity distributions at a cross section of the duct or the narrow chamber may thus be determined from the velocity distribution in an unconfined environment with the same jet conditions. The chamber walls represent mirrors or reflecting barriers. The parts of the velocity distribution for an unconfined environment, which reach beyond the mirrors, are "reflected and summed" with the interior portion of the velocity distribution. If these "reflected parts" in turn reach the opposite side of the chamber, they are again reflected and summed to the main central portion of velocity distribution. However, the summed-up distribution cannot be more uniform than the velocity distribution in the duct or the chamber for simple steady flow of the fluid through it. This mirror-type reflection is conceived with the walls being a reflecting barrier only and not the originator of new turbulence and head loss. This principle of mirror reflection is, therefore, valid only for those parts of large ducts or chambers, for which velocities along the walls and the friction resistance generated at the walls may be neglected for time-average velocity distribution as compared with the jet diffusion, expansion and deceleration.

Any jet diffusion in a long ducted environment must reach a final stage, or an equal flow rate and an equal velocity distribution at a cross section some distance from the orifice. This "mirror reflection" approach is valid only for that portion of the duct or the chamber which is located before this equilibrium cross section is reached.

The application of the "reflecting mirror" or "reflecting barrier" principle makes it appropriate to study only those cases of jet diffusion in which the environment is unconfined, or limited in such a way that the boundaries do not substantially affect that portion of the jet and environment which are involved in the study. In other words, boundaries of the environment are at such distances from the orifice that velocities are small along them relative to the velocity at the center of the jet, and that the region of experimental investigation is not affected by them. This criterium has been applied to experiments which were conducted in this study, so that only the case of diffusing jets in an unconfined environment with distant boundaries was investigated.

For the purpose of this study, jet contours were shaped in such a way that they allowed the environmental fluid to be entrained by the jet from all sides. The application of this principle will become clear by the description of experimental facilities and by the selection of the experimental fluid, as explained in details in the next chapter.

1.4 Establishing and established zones in jet diffusion.

When a jet leaves its orifice, the sudden change of boundary conditions forces the jet to expand. The contact between the jet fluid and the environmental fluid retards the jet by a decrease in momentum of the jet filaments because of the momentum transfer to the adjacent fluid. When this deceleration reaches the bulk of fluid on the jet-axis, the maximum velocity at the jet center begins to decrease appreciably with the distance. According to Albertson, Dai, Jensen and Rouse [27]* this initial portion of the jet is called the zone of flow establishment. It is actually a zone of flow transition and adjustment created by a sudden change in boundary conditions as it represents a jet core. Figure 1 serves as an illustration for definitions. The time-average velocity distribution at the orifice section A-B is nearly uniform, with the maximum velocity V_o, except at the edges of jet. This distribution depends on the length of the orifice nozzle and the conditions of flow in the approach to the orifice. The shorter the nozzle and the more regular the flow in the approach to the orifice, the more uniform is the velocity distribution at the orifice. The velocity distribution at the cross section D-D in the zone of establishment is composed of two parts: the jet core $\overline{12}$ with approximately a uniform velocity, V_o, and jet sides $\overline{23}$ with velocities which decrease with an increase of lateral distance from the jet-axis. The maximum or center velocity, V_m, at the cross section E-E is still very close to the orifice velocity, V_o. From the point C, in that cross section, the maximum velocity, V_m, begins to decrease appreciably with the relative distance X/B_o. Experiments made in the Iowa Study [27] show that for both a circular jet and a two-dimensional jet, V_m decreases along the jet axis in such a way that the experimentally obtained

---

*) As this reference will be mentioned several times, and as the study is made at the University of Iowa, it will be called here briefly "Iowa Study" [27].

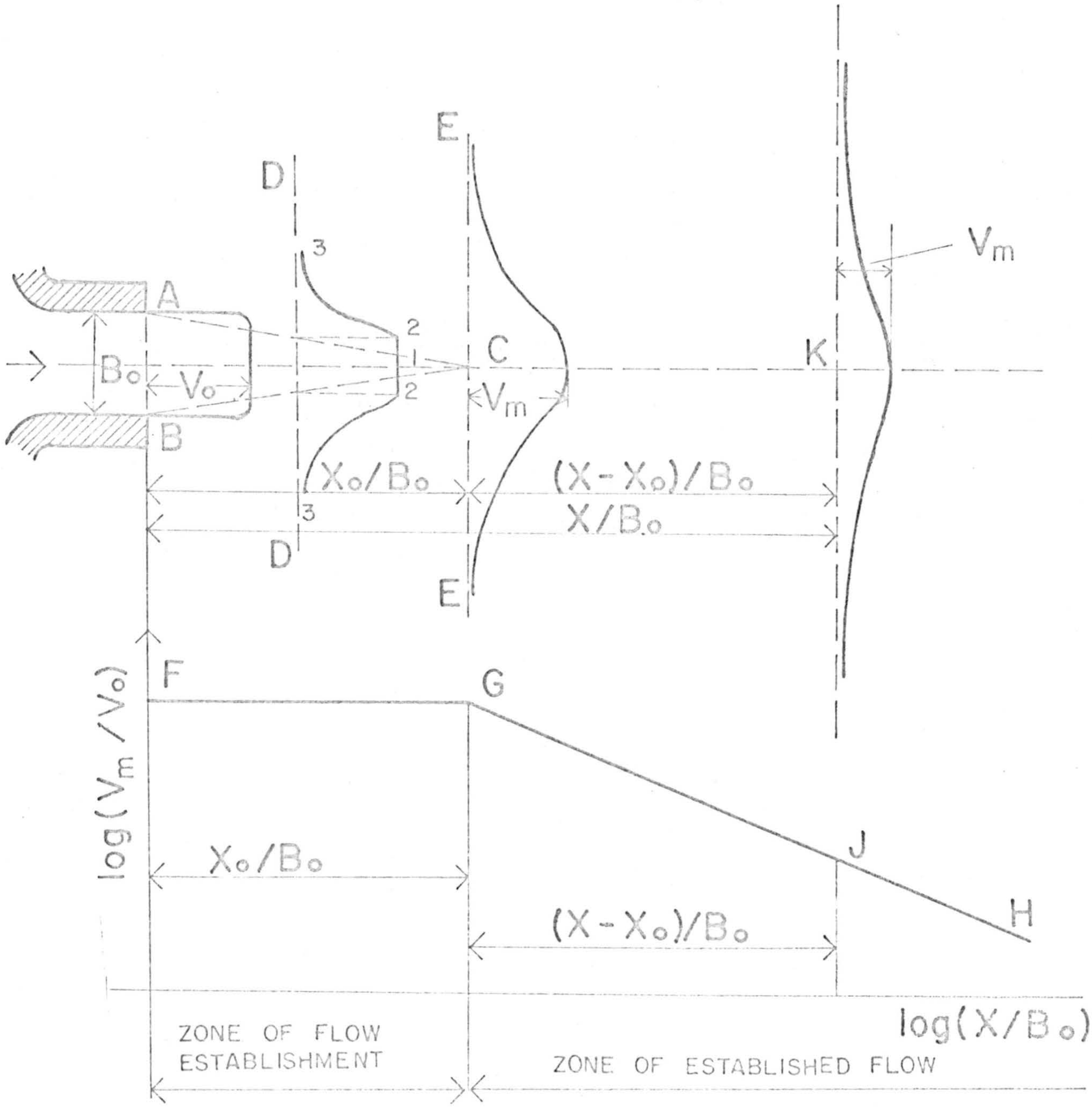

FIGURE 1 - DEFINITIONS OF ZONES OF ESTABLISHING AND ESTABLISHED FLOW FOR SLOT JETS.

relationship of log (V_m/V_o) versus log (X/B_o) or versus log (X/D_o), with B_o the slot width and D_o the diameter of circular jet, can be fitted, for each of the two, by a straight line, from X_o/B_o or X_o/D_o to the right, as shown in figure 1 by the line G-H. This line represents a hyperbolic decrease of the ratio V_m/V_o. The center velocity from $X = 0$ to $X = X_o$ is very nearly constant as shown by the line F-G in figure 1 from $X/B_o = 0$ to $X/B_o = X_o/B_o$. The value X_o is defined for the purposes of this study as the value of X at the intersection of lines FG and GH, which is the distance of the point C from the orifice. It does not mean that the central maximum velocity is exactly V_o at the point C. It is slightly lower than V_o as experiments show [27], but this somewhat decreased velocity, V_m, is still close to V_o.

The velocity at cross section EE is distributed approximately by Gaussian law (normal distribution function), as shown for a typical cross section at the point K. The zone to the right of cross section EE is called, in Iowa Study [27], the zone of established flow. It is the zone in which the jet expansion and velocity distributions are dependent only on the velocity distribution at the cross section EE. In other words, the velocity distribution at cross section EE is adjusted to the new boundary condition of jet, which is a contact of the jet with a fluid instead of a contact with the fixed boundary of the orifice nozzle. The cross section EE is called, in this study, the characteristic jet cross section. The velocity distribution at the characteristic cross section may be thought of as being created by jets with various velocities V_o and also with various orifice widths B_o in such a way that from that cross section V_m/V_o begins to decrease sharply.

The characteristic cross section may be thought of as the position in the jet diffusion at which the eddies created by the contact of jet fluid with environmental fluid (which eddies travel both inward and outward by the turbulent diffusion process) have penetrated to the central core of the jet. The exact position where the first low momentum eddy arrives from the contact of jet fluid and environmental fluid at the center line and starts to decelerate the core is subject to the probability laws of turbulent diffusion, because the probability that eddies, generated by contact of the two fluids and of various momenta reach the jet core increases with the distance. Therefore, a definition of position X_o/B_o cannot be thought of strictly as a fixed point. The definition of the characteristic cross section as an intersection of the two straight lines on graphs with log-log scales is only a practical definition in describing limits of the two zones in the jet diffusion by neglecting a third or a transitional zone which represents the transitional curve between the lines FG and GH in figure 1.

The zone of established flow is characterized by the process of diffusion which is similar in all cross sections. The jet diffusion causes central velocities to become smaller and the jet cross sectional area over a given range of velocities to become greater with an increase of the dimensionless distance X/B_o. The limit of an expanding jet, theoretically for very large values of X/B_o is represented by a very small velocity of a very large cross sectional coverage. However, the limiting condition for X/B_o being infinite has no practical meaning.

Two Japanese researchers, Sato [33] and Hom-ma [37], divide the total range of change of log (V_m/V_o) versus log (X/D_o) in four zones. The zones A and C coincide with the establishing zone and zone of established flow of the Iowa Study [27], while the zone B is the transition between the two. The zone D, in their study, represents the region to the extreme right of figure 1 with a faster deceleration than that of the zone C. By their estimate, this zone D is not reliable because of a limited number of experimental points in the zone. Furthermore, the points in this region coincide with the approach of jet to the boundaries normal to the jet, and some deceleration may be due also to this factor.

According to these two authors the zone limits for X_o/D_o are:

	Hom-ma	Sato
A Zone	0 - 4.8	
B Zone	4.8 - 8.2	4.55 - 12
C Zone	8.2 - 36.5	12 - 36
D Zone	36.5	

This study of slot jets will be based on the concept of only two zones, establishing and established, neglecting the transitional zone. The extreme right zone (D Zone) of fast deceleration will be regarded as uncertain.

The point G or C of figure 1 is evidently a function of the velocity distribution at the orifice cross section. Assuming a uniform velocity distribution at the orifice, the Iowa Study [27] gives $X_o/D_o = 6.2$ for the circular jets, and $X_o/B_o = 5.2$ for two-dimensional slot jets. As a square jet of the same orifice cross sectional area is assumed in this study as having approximately the same decelerating characteristics as the circular jet then area $B_o^2 = D_o^2 \ \pi/4$ which gives $D_o = 1.128 \ B_o$, so that the constant X_o/B_o for the square jet becomes approximately 7.0. Squire [30] finds this constant for circular jets to be $X_o/D_o = 6.5$.

Polyakov [50] finds that the point G of figure 1 depends on a form factor which describes the velocity distribution at the orifice.

Rosler and Bankoff [56] expand this analysis further. They obtain the constant X_o/B_o according to their studies and other studies [50] by using a different equation for V_m/V_o versus X/D_o than Iowa Study [27]. Because the difference is small, the constant cited in reference [56] may be compared with those in reference [27]. According to Rosler and Bankoff this constant is 6.52 for air jets and 6.58 for water jets. Corrsin [14] gives 5.3 and later [23] the value 6.55. Hinze [25] gives 6.35, and corrected by Rosler and Bankoff this value becomes 5.9. Polyakov's [50] value is 6.54, and Taylor's [34] 6.56. The above values, therefore, are in the range from 5.3 or better from 5.9 to 6.58.

Baines [discussion, reference 27] shows that the position of X_o/D_o is dependent on two other factors: Reynolds number, R_e, and the method of producing fluid circulation through the orifice. According to his analysis of both his data [21, 17] and data of other authors [14, 19 and some others], the values of X_o/D_o for the case of blower type air circulation range from 5.0 for $R_e \cong 10^4$ to 7.0 for $R_e \cong 7 \times 10^4$, and for an air-line assembly from 5.0 for $R_e \cong 10^4$ to 6.5 for $R_e \cong 10^5$. He has shown that the blower type air supply has about twice the turbulence level of an air-line assembly, because the blower blades create additional turbulence and vorticity which persist beyond the orifice in the jet itself. He describes in detail [27] the two cases of V_m/V_o versus X/D_o for two R_e: $R_e = 2.1 \times 10^4$ with $X_o/D_o = 5.75$ and $R_e = 7 \times 10^4$ with $X_o/D_o = 6.85$.

The above differences in the values X_o/D_o or X_o/B_o depend, therefore, on the accuracy of velocity measurements, on the definition of the constant itself, on differences in Reynolds numbers used in experiments, and on various assemblies for air or water supply. For the purposes of comparison in this study, the approach of the Iowa Study [27] will be used, and the constants will be 5.2, 6.2 and 7.0 for two-dimensional slot jet of infinite length, circular jet and square jet, respectively; however, these constants will be considered as approximations only.

1.5 Hypotheses underlying the theory of jet diffusion.

Analytical expressions developed theoretically for the flow pattern of diffusing free submerged jets are based on the following assumptions [27]: (1) Pressure inside the system of jet liquid and environmental liquid is hydrostatically distributed vertically throughout the flow region. In an environment of a very light fluid, like the atmosphere, the pressure inside the air jet and around it may be considered as constant; (2) The process of jet expansion and deceleration in turbulent flow is dynamically similar; and (3) The time-average velocity components parallel to the jet-axis within the jet expansion region vary approximately according to the Gaussian probability density function at a cross section perpendicular to the jet-axis in the region of established flow.

The first assumption of pressure being hydrostatically distributed vertically for liquids or constant inside the moving fluid for gases is shown to be valid [27 and discussions] for unconfined environments and is an approximation for confined regions. The retarding jet is usually associated in confined regions with a conversion of a part of kinetic energy into potential energy (pressure), and this phenomenon is not likely to support strictly the hypothesis of hydrostatically distributed pressures for liquids or constant pressures for gases in confined environments.

The second assumption of dynamically similar processes implies that the ratio of main forces acting on the moving fluid does not change with the change of jet dimensions for a given jet orifice type or jet velocity at the orifice, as long as the flow is either laminar or turbulent throughout the region of investigation. This also implies that the similitude is obtained regardless of the selection of fluid as long as the fluids, such as air and water, are of moderately low viscosity. However, because the flow regime at distant regions of environment is laminar while the main region of jet expansion and diffusion is in a turbulent regime, this assumption of dynamically similar processes must be restricted to the regions of the same flow regime.

The third assumption of time-average velocity being distributed by Gaussian law in a cross section is still somewhat controversial. The velocity distribution in a cross section taken perpendicular to the jet-axis depends on the type of jet orifice. The cross section plane for the study of velocity distribution is usually taken perpendicular to the jet-axis with the velocity distributions in that plane including the point on the jet-axis; however, many of the traverses in that plane for which the velocity distribution is investigated in this study do not include the point on the jet-axis. The experimental evidence in several experimentations [1, 2, 11, 13, 16, 17, 19, 27, 55, and others] and in experiments made for this study shows that for the jet area sufficiently distant from the orifice, the hypothesis of Gaussian or normal distribution for time-average velocities along a traverse is acceptable from the practical point of view. The accuracy in determination of time-average velocity is usually such (the accuracy being a function of the time-average velocity measuring device, the precision in locating the point of measurement, and variation in Reynolds numbers) that differences between a fitted normal function to the determined time-average velocities and the hypothetical true distribution can hardly be discriminated, at least in the region of large velocities.

It is clear from the physical aspects of jet diffusion that the velocity at the tails of its distribution becomes zero at finite distances from the jet-axis, while the normal distribution implies velocities being zero only at infinity [11]. The fit of a normal function to measured velocities shows that the main departure is at the very tails, especially for cross sections not far from the characteristic cross section (EE in figure 1). Several authors [27, discussion] have shown that this hypothesis of Gaussian velocity distributions is not necessary in the derivation of equations for diffusion of the submerged jets. However, this hypothesis will be used in this study simply to compute parameters of the velocity distributions based on the fit of a normal function to experimental data.

The principle used in the theoretical development of the time-average velocity distribution of diffusing jets, is that of constancy of flow momentum. The flow momentum in cross sections normal to the jet-axis does not change from one cross section to the next. In other words, the momentum flux is constant for all normal sections of a given flow pattern. This is valid only for unconfined environments, for which there are no external forces available to change the momentum flux.

Several hypotheses for the jet diffusion process such as the mixing length concept [1, 2, 4, 11, 13], vorticity transport concept and constant eddy viscosity across any cross section of the diffusing zones [6, 7, 8, 9, 12] and other hypotheses [18] have been used in the past to develop theoretically the velocity distribution pattern in a free submerged and diffusing jet. The comparison of theoretical and experimental velocity distributions has always shown a gap which has caused questioning of the validity of assumptions underlying the theoretical equations. However, the detailed and careful measurements by several authors [14, 20, 54, 55] have produced results which have led to better theoretical derivations, and thus to a better bridge between analytical and experimental results.

It is not known to the author of this study, at the present time, whether the probability approach in the form of random walk has ever been attempted in theoretically deriving the time-average velocity distributions in diffusing free submerged jets. It has been applied to velocity distributions in pipes and channels with relatively good success.

The jet at the orifice cross section suddenly changes boundary conditions in such a way that the "absorbing barrier" of the duct or the pipe walls, through which the jet enters the environment, disappears. The transitional probabilities of fluid passing laterally from one space element (Δx, Δy, Δz) to the adjacent ones are not zero as in the case for those elements which are beyond the absorbing barriers. It is expected that the random walk hypothesis of jet diffusion, with transitional probabilities adequately defined or determined, would show a surprising similarity with the time-average velocity distributions obtained by accurate experiments. As the use of the digital computer is handy, the integration of random walk equations poses no difficult problem.

1.6 Decrease of maximum jet velocity with distance.

This report is primarily oriented to solving practical problems of slot jet distributions for slot orifices with finite length-width ratios. Therefore, it seems appropriate to start with the information available in the literature for circular jets and two-dimensional slot jets.

The results of these jet investigations usually have been represented as relationships of dimensionless ratios. One such ratio is the V_m/V_o, where V_m and V_o are as defined in figure 1. Another ratio is X/D_o or X/B_o, the relative distance from the orifice in terms of the characteristic orifice dimension. The literature gives both relationships, either as,

$$\frac{V_o}{V_m} = f_1 \ (\eta)$$

or as

$$\frac{V_m}{V_o} = f_2 \ (\eta)$$

where $\eta = X/D_o$

or $\eta = X/B_o$

The first form gives V_o/V_m as going to infinity with an increase of η while the second form gives V_m/V_o as conveying to zero with an increase of η. As the velocity distribution in jet diffusion is primarily concerned with the velocity decrease with distance, the second form of representation appears more convenient for practical purposes; therefore, it is used in this study.

The Iowa Study [27] clearly revealed that one expression is valid for the decrease of the maximum velocity along the jet-axis for the two-dimensional (infinite length) slot jet, and another expression is valid for the circular jet. The relative maximum velocity V_m/V_o decreases along the jet-axis of the two-dimensional slot jet [27, equation (39)] as

$$\frac{V_m}{V_o} \sqrt{\frac{X}{B_o}} = 2.28 \tag{1}$$

while V_m/V_o for a circular jet [27, equation (47)] decreases as

$$\frac{V_m}{V_o} \ \frac{X}{D_o} = 6.2 \tag{2}$$

A log-log plot of these two equations is represented in figure 2 as two straight lines. This comparison shows that the "carry of fluid" in circular jets is less efficient than in the case of a two-dimensional slot jet, if the diameter of a circular jet is equal to the slot width of the two-dimensional slot jet. As an example, for $X/B_o = X/D_o = 100$, the ratios V_m/V_o are 0.228 and 0.062 for the two-dimensional slot jet and the circular jet, respectively. This essential difference between the two types of jet makes them different in their application. However, if D_o and B_o are equal, much more fluid will pass through the orifice for two-dimensional jets than for circular jets. Assuming that the orifice flow rate and efflux velocity are equal for both types of jets, the circular jet presents quite a different picture for jet penetration, as it is shown later in this text.

Assuming that a square slot has the same area as the circular jet, or $D_o = 1.128\ B_o$, it is expected that for a sufficient distance X from the orifice the two jets will have very similar velocity distributions. Equation (2) in the case of square jets becomes

$$\frac{V_m}{V_o} \quad \frac{X}{B_o} = 7.0 \tag{3}$$

The question now arises, what will be the relationship $V_m/V_o = f\ (X/B_o)$ as the ratio L_o/B_o of slot orifice changes from 1 to infinity by keeping the area $A = L_o\ B_o$ constant. For a very large ratio L_o/B_o, the slot jet approximates, at least in its central cross section through the jet-axis and perpendicular to the long side of the orifice, the two-dimensional jet with $V_m/V_o = f\ (X/B_o)$ given by equation (1). An equation of hyperbolic type for diffusing slot jets is needed for practical purposes, which contains the ratio L_o/B_o as a

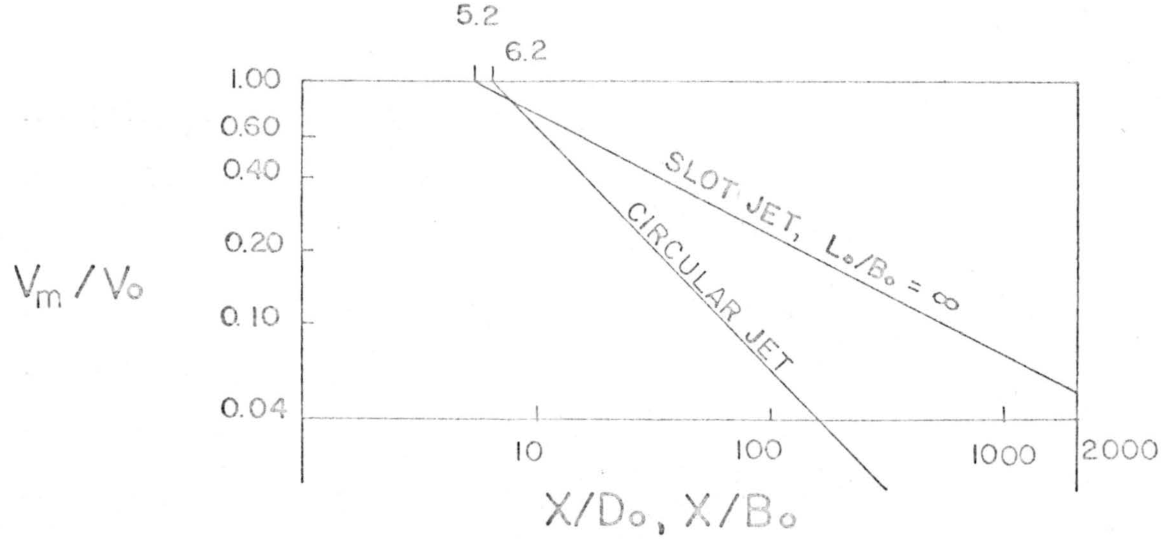

FIGURE 2 - THE DECELERATION OF CIRCULAR AND TWO-DIMENSIONAL SLOT JET, AS OBTAINED IN THE IOWA STUDY [27].

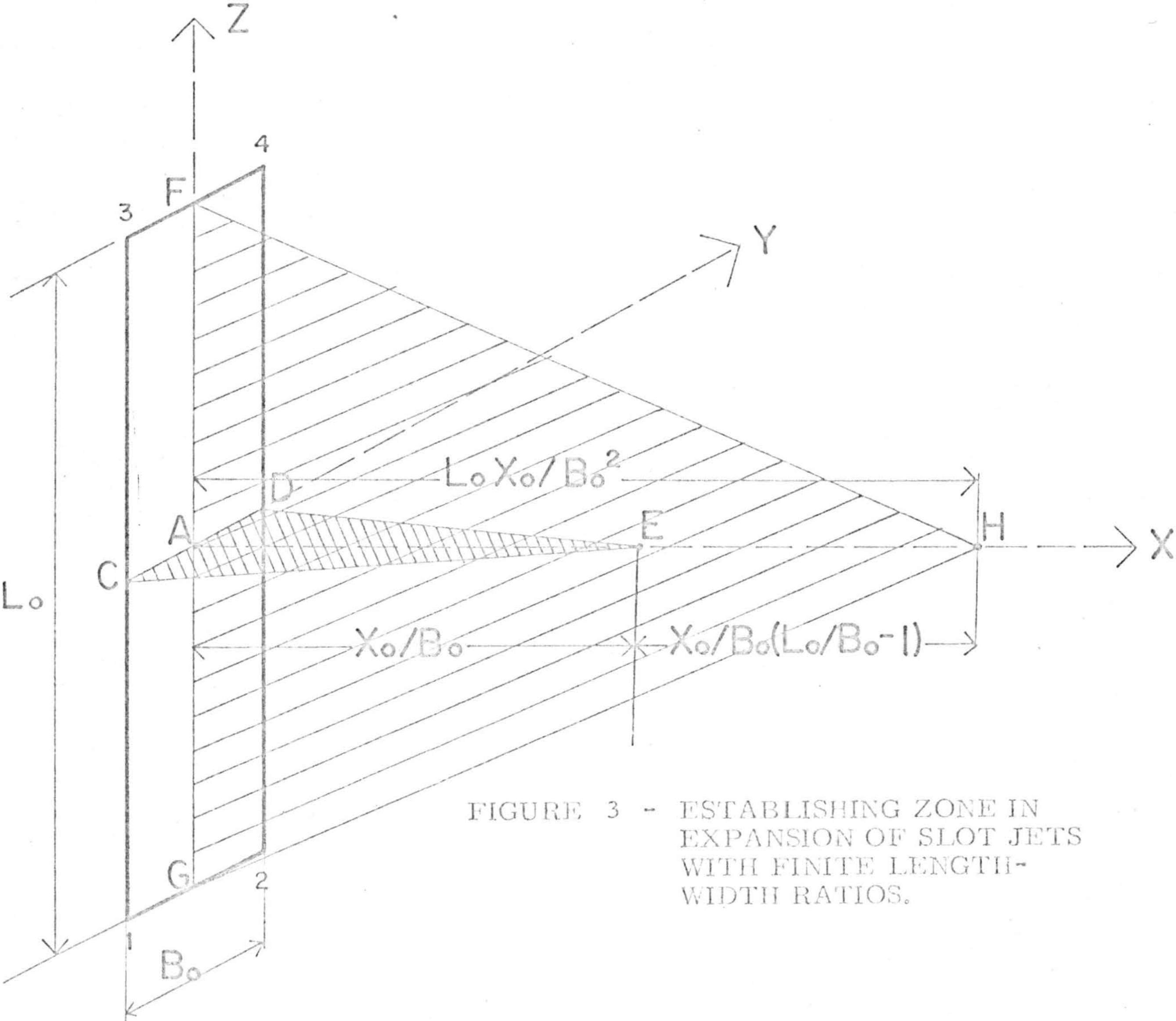

FIGURE 3 - ESTABLISHING ZONE IN EXPANSION OF SLOT JETS WITH FINITE LENGTH-WIDTH RATIOS.

parameter. The main objective of experiments conducted for this study was a search for that expression which contains the ratio L_o/B_o for slot jets of finite dimensions L_o and B_o.

A slot jet having finite values L_o and B_o, or a relatively small ratio L_o/B_o, has an establishing zone which is affected on two sides by boundary effects, as it is shown in figure 3. The maximum velocity along the jet-axis, which is V_o, is not much affected by jet expansion in the triangle CDE in the horizontal plane, and the effects of sides $\overline{12}$ and $\overline{34}$ are not felt significantly in the triangle FGH in the vertical plane. The velocity ratio V_m/V_o stays close to unity along the jet-axis for the distance AE. From E to H the relationship $V_m/V_o = f(X/B_o)$ should be approximately the same as for a two-dimensional slot jet of infinite length, as described by equations (1) and (3). The distance of the point H from the efflux orifice is approximately

$$\frac{L_o X_o}{B_o B_o} = \frac{L_o X_o}{B_o^2} \tag{4}$$

Effects of the sides $\overline{12}$ and $\overline{34}$ on the relationship $V_m/V_o = f(X/B_o)$ are expected to depend thus on the ratio L_o/B_o.

1.7 <u>A summary from literature of flow pattern equations for circular jets and two-dimensional infinite slot jets.</u>

The dimensionless ratios V/V_o, Q/Q_o, M/M_o, E/E_o and σ/X describe the flow patterns at different positions in the diffusing jets. The values V, Q, M, E, and σ refer to velocity, flow rate, momentum, energy and standard deviation of the velocity distribution at different cross sections perpendicular to the jet-axis, respectively, while V_o, Q_o, M_o, and E_o refer to the same magnitudes at the orifice of jet efflux. The velocity V is the velocity component in the direction of jet-axis at any point in the diffusing jet field. Of special importance is the maximum velocity V_m along the jet-axis, because its ratio V_m/V_o which decreases with distance is usually taken as a measure of the deceleration of the jet.

The coordinate axis X will be assumed always in the direction of jet-axis, the Y axis normal to X and to long side of the slot, and Z axis along the long axis of the slot, normal to X axis. The origin is at the center of the orifice (see figure 3).

For the two-dimensional slot jets, in the zone of established flow, the Iowa Study [27] gives the normal distribution of velocity V_x as

$$\log_{10} \frac{V_x}{V_o} \sqrt{\frac{X}{B_o}} = 0.36 - 1.84 \frac{Y^2}{X^2} \tag{5}$$

This equation becomes equation (1) for $V_x = V_m$ and $Y = 0$.

The volume flux ratio Q/Q_o is given as

$$\frac{Q}{Q_o} = 0.62 \sqrt{\frac{X}{B_o}} \tag{6}$$

The momentum ratio is unity, or

$$\frac{M}{M_o} = 1 \tag{7}$$

and the energy flux ratio is

$$\frac{E}{E_o} = 1.86 \sqrt{\frac{B_o}{X}} \tag{8}$$

The ratios Q/Q_o, M/M_o, and E/E_o are graphed in figure 4 for the

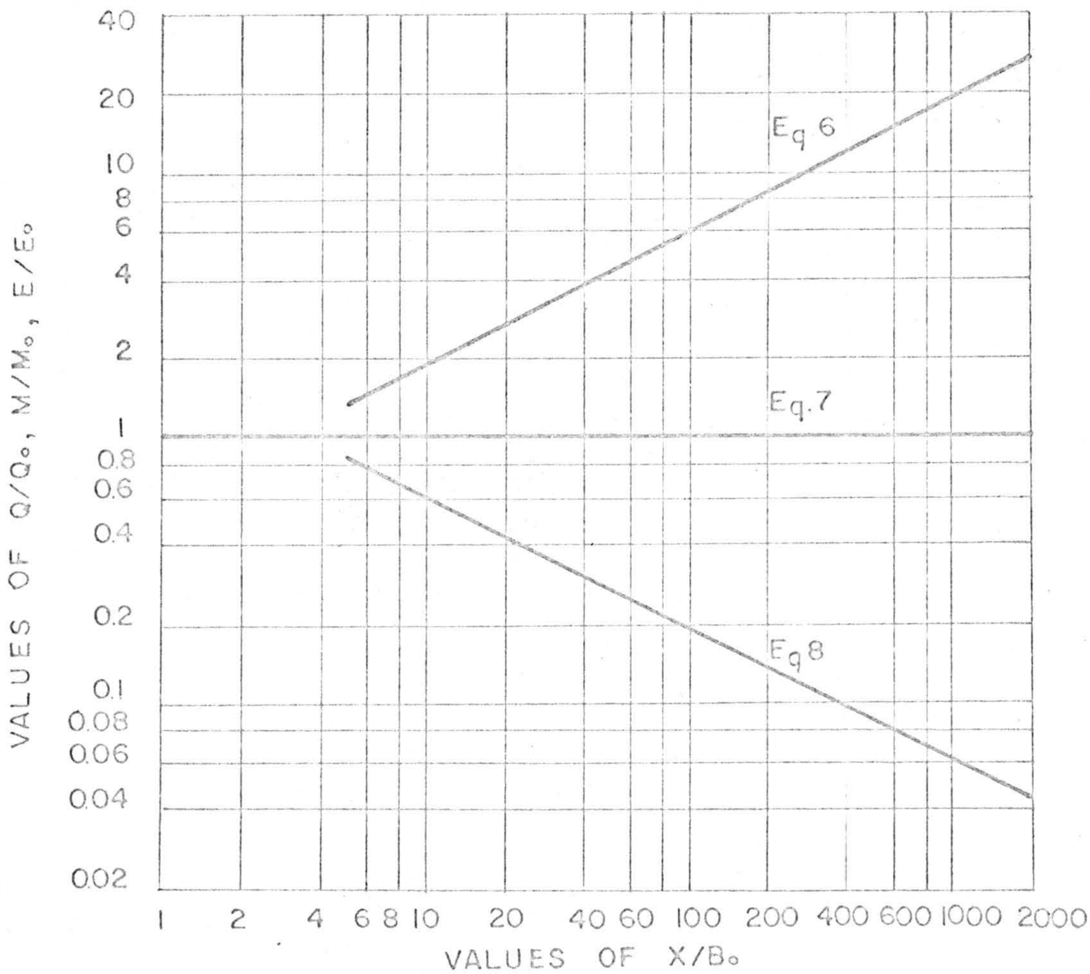

FIGURE 4 - DISTRIBUTION OF RELATIVE VOLUME, MOMENTUM, AND ENERGY FLUX FOR SLOT JET IN ZONE OF ESTABLISHED FLOW.

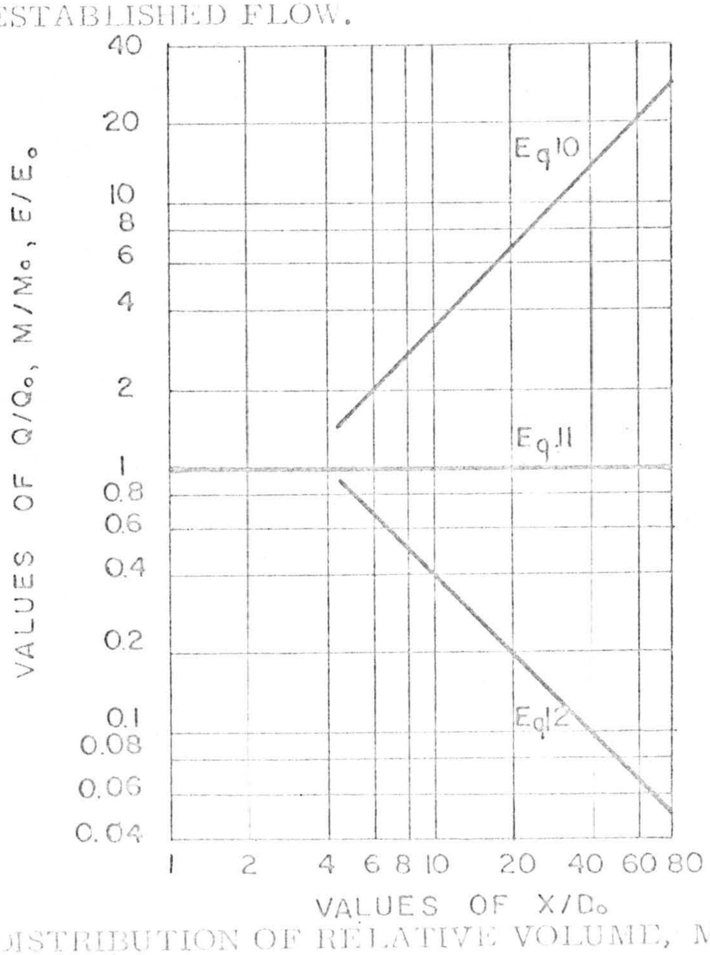

FIGURE 5 - DISTRIBUTION OF RELATIVE VOLUME, MOMENTUM, AND ENERGY FLUX FOR CIRCULAR JET IN ZONE OF ESTABLISHED FLOW.

two-dimensional jet.

For the circular jet, in the zone of established flow, the above equations (equations 5-8) are:

$$\log_{10} \frac{V_x}{V_o} \frac{X}{D_o} = 0.79 - 33 \frac{r^2}{x^2} \tag{9}$$

where r is radial distance from the jet-axis, which replaces Y in equation (5). For $r = 0$, equation (9) becomes equation (2). For the circular jets

$$\frac{Q}{Q_o} = 0.32 \frac{X}{D_o} \tag{10}$$

$$\frac{M}{M_o} = 1 \tag{11}$$

and

$$\frac{E}{E_o} = 4.1 \frac{D_o}{X} \tag{12}$$

The ratios Q/Q_o, M/M_o, and E/E_o as functions of X/D_o for the circular jet are given in figure 5.

The dimensional analysis [27] shows that ratios V_m/V_o, Q/Q_o, M/M_o, and E/E_o may be expressed as various functions of X/B_o for two-dimensional jets, and of X/D_o for circular jets. For slot jets of various L_o/B_o ratios, the above equations should include this second dimensionless ratio. The velocity ratio, V/V_o, includes also the ratios Y/X and Z/X for slot jets, and r/X for circular jets, and they determine the position of points to which the ratio V/V_o refers.

According to the Iowa Study [27] the ratio of the standard deviation, σ, of the velocity distribution in a cross section to the distance from orifice is a constant for the two-dimensional jet and for the circular jet, or

$$\frac{\sigma}{X} = C \tag{13}$$

in order to satisfy the condition of dynamic similarity, and has a value of $C = 0.109$ for the two-dimensional jet, and $C = 0.081$ for the round jet. However, according to S. Corrsin [27, discussion] the assumption of dynamic similarity alone, by the authors of the Iowa Study, does not give the linear spread of a jet, and σ/X = constant cannot simply be assumed. The authors of the Iowa Study in their closing of discussion revised the statement by asserting that "the constancy of the momentum flux together with the similarity of the velocity profiles at successive sections will be found to require that $\sigma/X = C$. That is, the jet will spread at a linear rate defined by the constant C." This problem, whether the two-dimensional or circular jets expand linearly, is still to be finally decided by more accurate experiments.

1.8 Jets of miscible but different jet and environmental fluids.

The jet fluid and the environmental fluid very often have a small difference in properties and are miscible. Usually, the gravitational forces appear in that case which affect jet patterns. This study is concerned neither with this case, nor with the case in which a jet enters a moving stream instead of an environment with the fluid at rest. However, some references for those cases are given at the end of this text [15, 24, 26, 45, 46, 47, 48, 49, 52, 53].

1.9 Applications.

The theory of diffusing jets is applied to many engineering problems. Among the most important are those applications which utilize one or another of the jet properties, such as the capacity of the jet for energy dissipation; rapid mixing of fluids; replacement of molecular convective diffusion by a turbulent diffusion; stirring of fluids which are inaccessible for mechanical stirring; entrainment of large masses of a fluid in a given direction; recuperation of kinetic energy of jets entering a ducted flow; and similar applications.

Often there are advantages, structural or otherwise, for using slot jets of various length-width ratios instead of the circular or, two-dimensional jets. From these practical aspects, the study of slot jets with slots of finite length-width ratios is considered attractive and useful. Therefore, the stress in this study is on those characteristics of slot jets which are necessary for engineering applications.

CHAPTER II

2. EXPERIMENTAL FACILITIES AND EXPERIMENTS

2.1 Selection of experimental fluid.

Both water and air were considered for use as the experimental fluid for this study. Three alternative facilities were studied for water as the experimental fluid: (a) The Indoor Hydraulics Laboratory, using sumps below the laboratory floor as the environment for investigation of free submerged water jets; (b) Outdoor Facilities, namely the new pumping station in the Outdoor Hydraulics and Hydrologic Laboratory, and the use of College Lake as the environment for investigation of free submerged water jets; and (c) Horsetooth Reservoir which is near the Hydraulics Laboratory, as the environment, with the improvisation of a pumping facility on a raft or boat. After a detailed study, the conclusion was made that all three alternatives with water as the experimental fluid would result in a more expensive, and a more time consuming approach than the use of air as the experimental fluid. Stratification of water according to water temperature both in the lake and in the reservoir was another adverse factor in this analysis. Since the sumps in the Indoor Hydraulics Laboratory are limited in content, they would represent a confined region rather than a practically unconfined environment.

The availability of a 50 h.p. centrifugal air blower and the large space inside the Indoor Hydraulics Laboratory, as well as the ease with which the experiments could be performed, were the main factors in deciding to use air as the experimental fluid for the investigation of diffusion of free submerged slot jets of various length-width ratios.

The similitude of fluid mechanics phenomena between air and water in highly turbulent flow has been long established. This is especially valid for the same range of Reynolds numbers of both fluids. As the air velocities used in this investigation were very large at the orifice (between 180 and 520 f. p. s.), the Reynolds numbers were relatively large, so that the similitude of the diffusion processes for the air and the water in this range of Reynolds numbers was assured.

The experiments conducted in the Hydraulic Institute of the University of the Iowa Study [27], by using air as the experimental fluid, and the experiments conducted in Japan [33, 39] and Northwestern University, Evanston, Illinois [56] by using both water and air as experimental fluids do not show a substantial difference in results between the use of water and of air in these investigations. Much of these differences may be attributed to variations in Reynolds numbers of the experimental runs, to errors in the measuring instruments, and to experimental techniques rather than to the use of different fluids.

The effect of Reynolds numbers on the diffusion process in a fully developed turbulent flow is still a somewhat unclear subject as was noted above. Measuring techniques are still not perfected to such a degree as to determine uniquely how the change of Reynolds number affects the diffusion process, and the above equations for the change of V/V_o, Q/Q_o, and E/E_o with the distance X/B_o or X/D_o.

After a detailed analysis of all aspects of using water and/or air as the experimental fluid, the decision was made to use air as the fluid in the investigation.

2. 2 Experimental facilities.

Experimental facilities were installed in the Indoor Hydraulics Laboratory at the Engineering Research Center of Colorado State University, Fort Collins, Colorado. They consisted of a 50 h.p. centrifugal air blower, two scaffolds, carriage equipment for moving and positioning the Pitot tube, and measuring and recording apparatus. Figure 6 shows these facilities in a top view, figure 7 shows a North-South cross sectional view, and figure 8 shows an East-West cross sectional view; all these figures are schematic representation, but the main features of the facilities are represented.

The air supplied by the blower was conducted through a transition from the circular blower outlet of 14" diameter to the square entrance of an elbow with 14" sides, and then through the elbow to the orifice nozzle. This elbow transition is show in figure 9. The square cross section and 90 degree elbow with four turning vanes was used to guide the air stream in such a way that the velocity profile of the air at the approach to the orifice nozzle was as symmetrical as practically feasible, and directed vertically upwards. The top of the elbow, where the guiding vanes end, continues as a straight vertical box 12" long, with a square cross section 14" by 14", as shown in figures 6 and 9. This box was closed from above by a top cover with the nozzle mounted in its center, as it is shown in figure 10. In this way, the air jet was directed vertically upwards. A typical nozzle cross section is shown in figure 11. This arrangement enabled the air flow to be changed in direction from the horizontal inlet to the vertical outlet, and to be concentrated symmetrically through the nozzles of small cross section.

Flow rates were governed by regulating the inlet area of the blower. The completely open area gave the maximum flow rate. A board with holes in it, covering the inlet, enabled the regulation of flow rate by opening a given number of holes in the board.

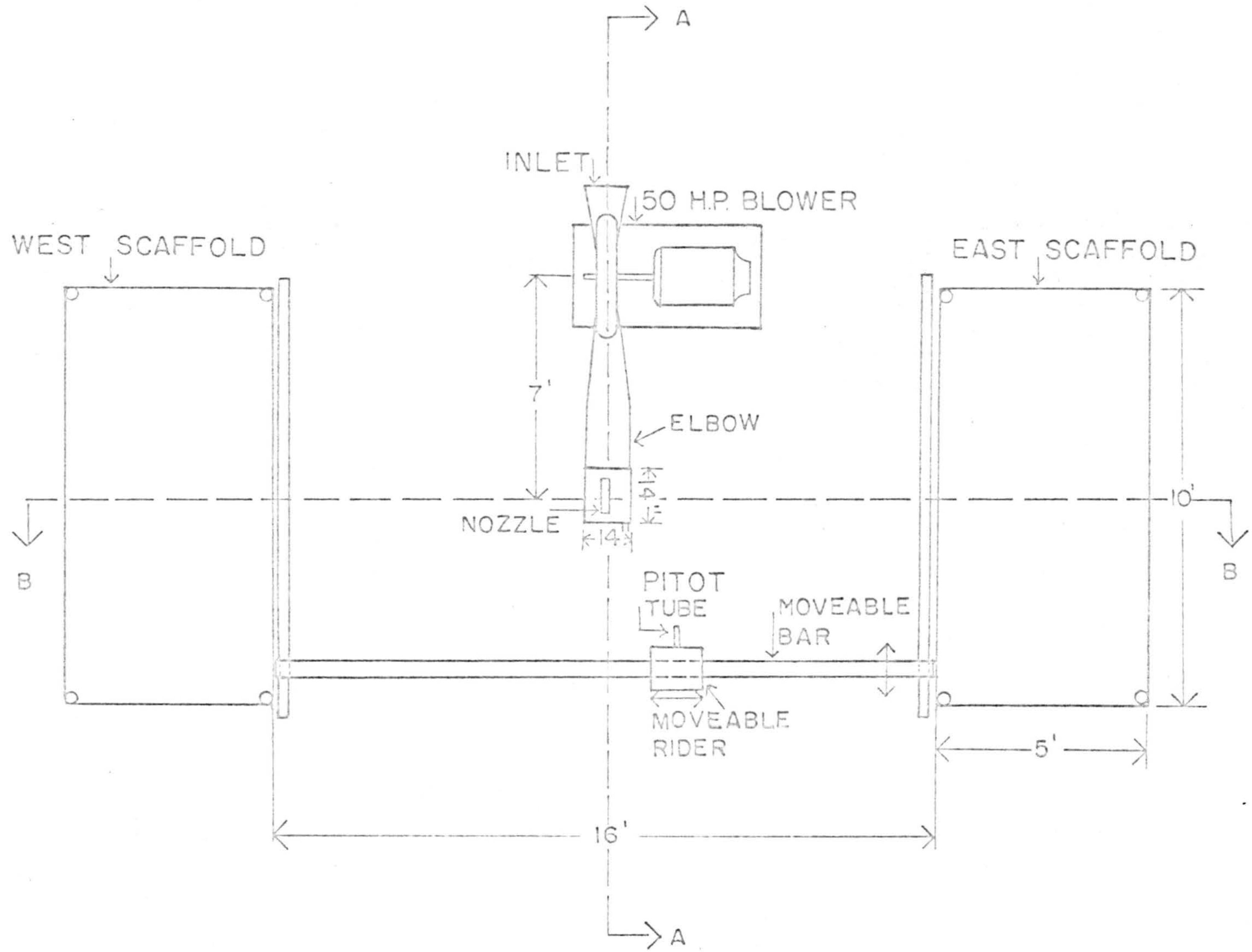

FIGURE 6 - EXPERIMENTAL FACILITIES, TOP VIEW

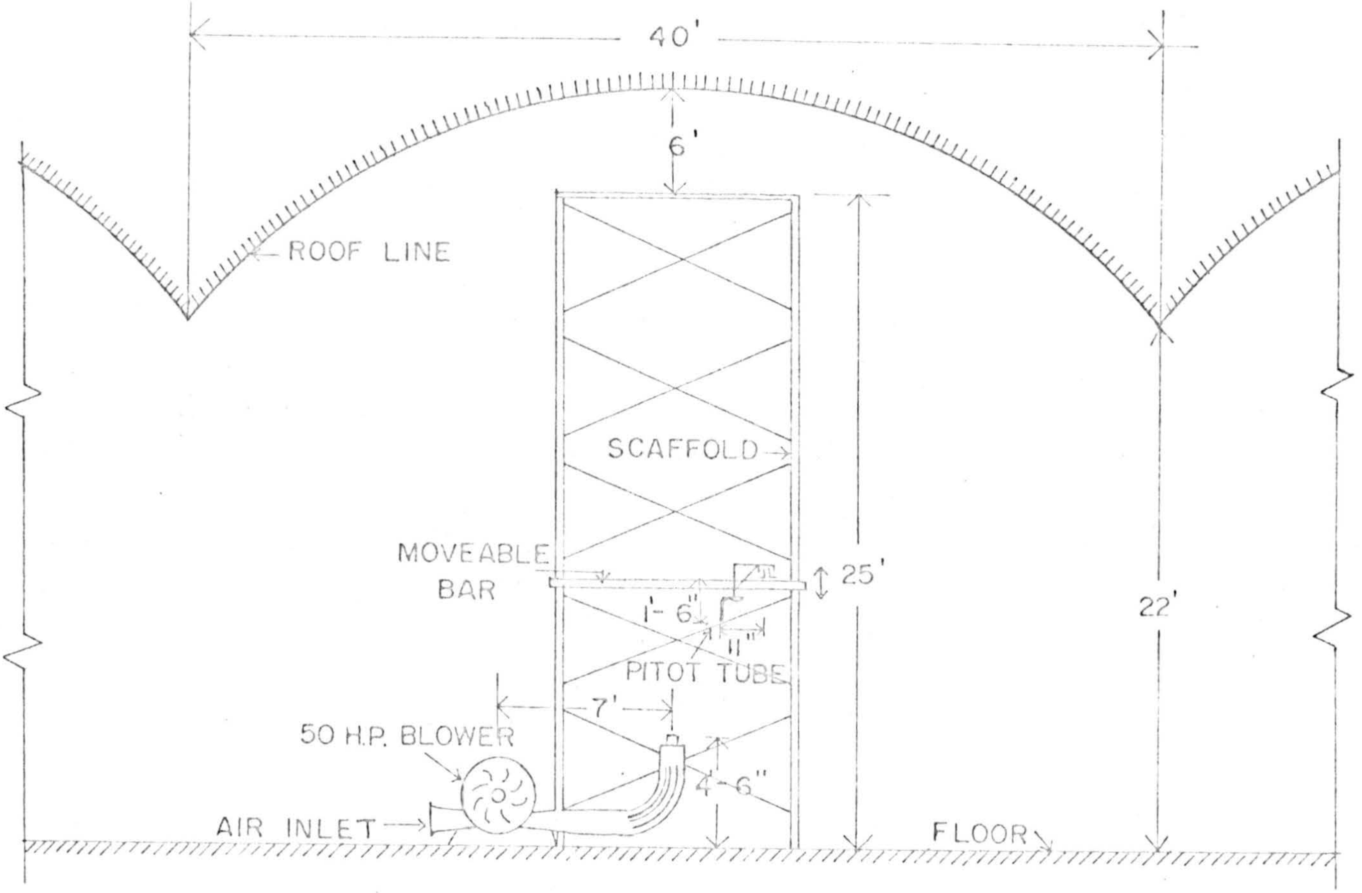

FIGURE 7 - NORTH-SOUTH CROSS SECTION, A-A.

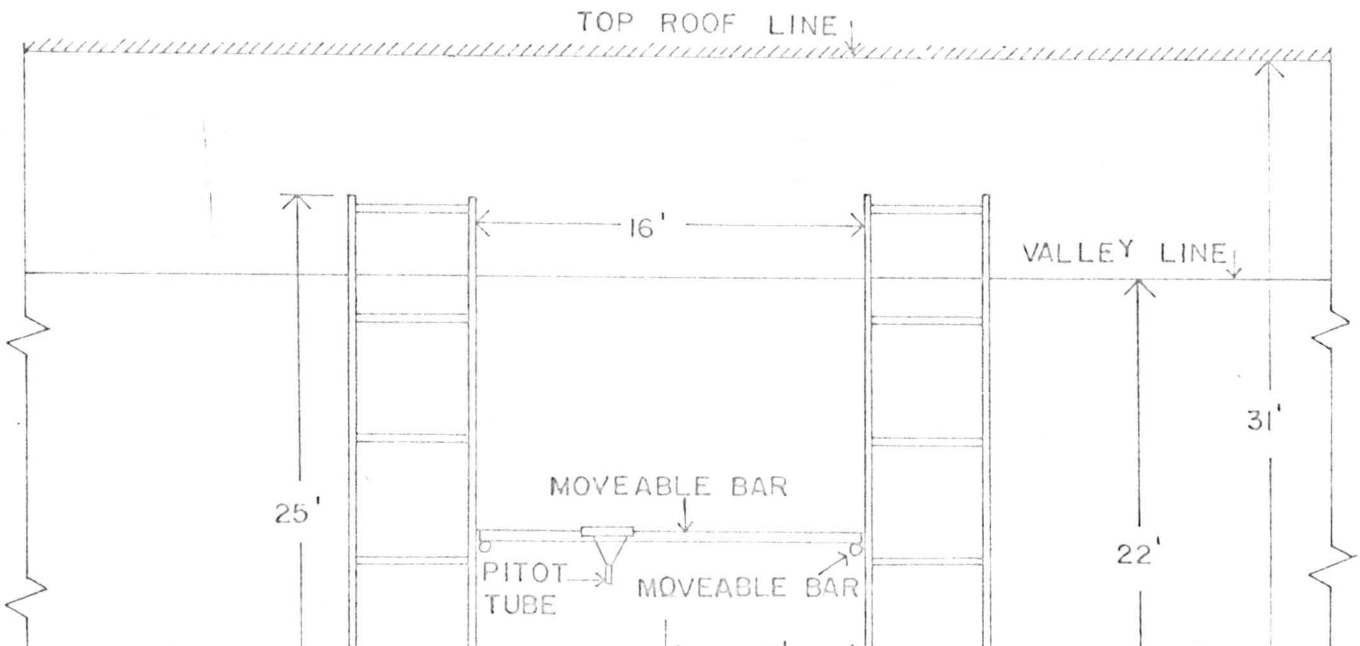

FIGURE 8 - EAST-WEST CROSS SECTION, B-B.

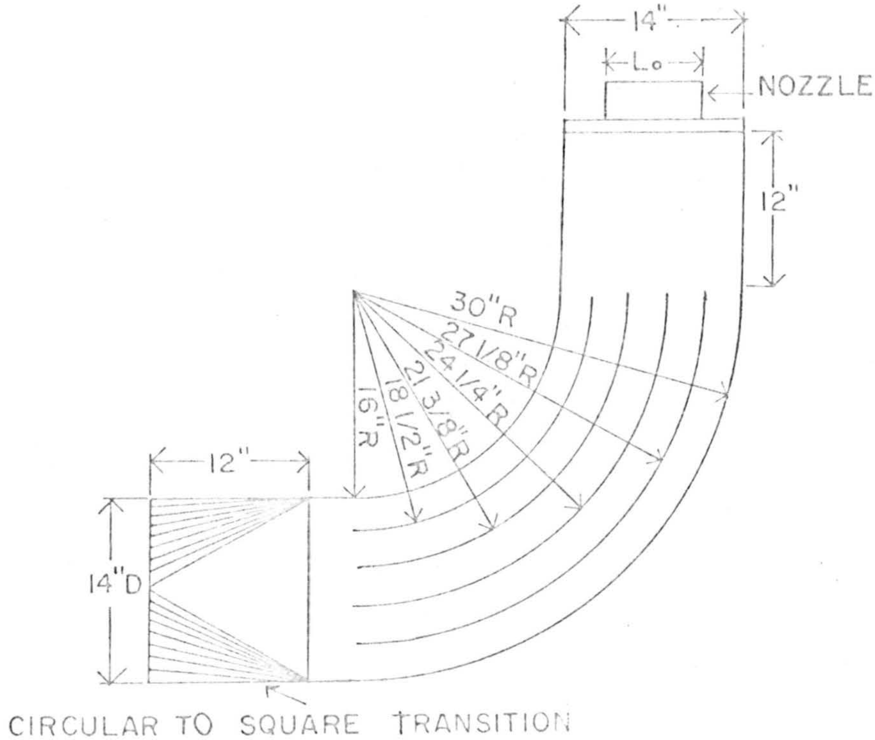

FIGURE 9 - TRANSITION FROM THE BLOWER TO ELBOW, ELBOW WITH GUIDING VANES, AND ORIFICE NOZZLE.

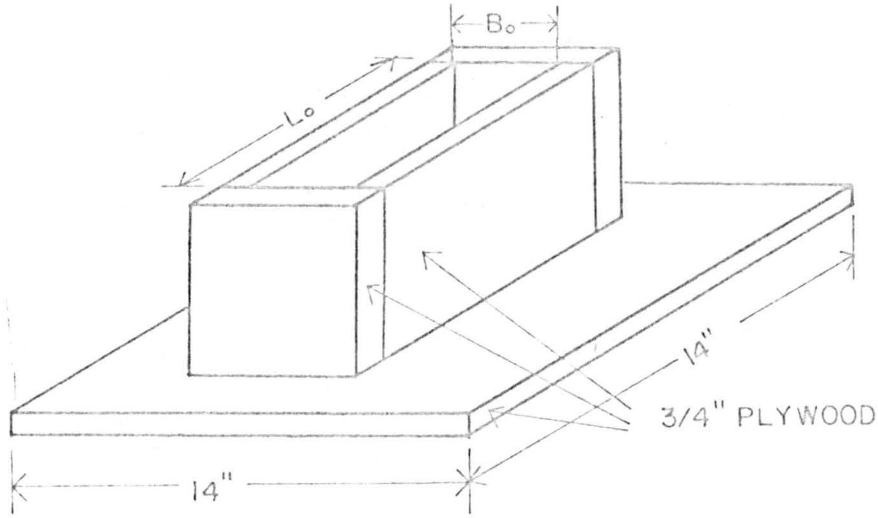

FIGURE 10 - TYPICAL NOZZLE IN THE TOP COVER OF THE ELBOW.

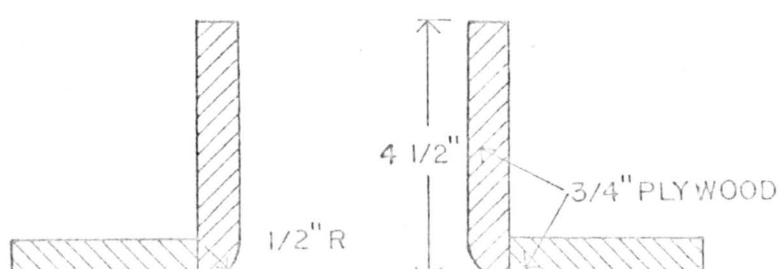

FIGURE 11 - TYPICAL NOZZLE CROSS SECTION.

The high speed centrifugal blower heated the air from an ambient temperature of 80-88 degrees to 150-170 degrees. A cooling system was necessary to substantially decrease the temperature difference between the air of the jet and the environmental air. In order to cool the air jet, the lower part of the blower was set in a "water bath", which consisted of a wooden box with cold water circulating through it. This cooling device lowered the air jet temperature substantially, but not sufficiently. The spray of water on the upper part of the blower further decreased the air jet temperature to about 15 degrees above the ambient temperature. This temperature difference, however, resulted in a buoyancy force directed upwards along the jet. This force is, therefore, a source of error in measuring the velocity distribution at various elevations above the nozzle orifice. However, two factors make this error small: first, the jet outlet velocities were very large (180-520 f.p.s.) so that the velocities caused by the buoyancy force are relatively small in comparison with the jet velocities at least for a couple of feet above the nozzle orifice; and second, the mixing of the jet air and the environmental air progresses fast along the jet-axis, so that the buoyancy force decreases rapidly with the distance from the jet orifice until at approximately two feet the air temperature was nearly the same as the ambient temperature.

Ten rectangular nozzles with varying length-width ratios were used. Five had an area of 1.844 square inches with length-width ratios of 1.00, 4.93, 13.5, 30.7, and 54.2. The other five had an area of 1.000 square inches and length-width ratios of 1.00, 4.00, 16.00, 45.8 and 94.0. One round nozzle was also used for comparison with the square nozzles: Its diameter was 1.125 inches. The nozzles were constructed from 3/4 inch plywood as shown in figure 11 and were coated on the inside with fiberglass to make a smooth surface.

Scaffolding was used to fasten the Pitot tube carriage vertically, and to provide a means for personnel to work above the nozzle. The carriage assembly was constructed in such a manner as to allow the Pitot tube to be moved in all three directions: vertically by moving the position of the main carriage, horizontally in a North-South direction, by moving the carriage of the Pitot tube rider; and, horizontally, in an East-West direction, by moving the Pitot tube rider along the carriage for an exact position of the Pitot tube.

The doors of the Hydraulics Laboratory were always closed during the experiments, which usually took place outside the regular working hours. This arrangement was necessary for two reasons: to enable the doors to be closed during the experiments and to avoid any major change in environmental air temperature because of the outside daily temperature fluctuations, and to assure a convenient electric energy supply with a minimum local interference in the frequency of the electric power supply.

Regardless of the precautions taken for avoiding air currents by closing the doors, there were some low speed air currents inside the laboratory during the experiments. These currents and the difficulty of fixing the nozzles with their X axis exactly vertical, as well as the effects of blower blades made the jet expansion such that the point of maximum velocity sometimes deviated slightly from the vertical line through the nozzle center. However, these deviations were relatively small, as it will be shown later in the discussion of data analysis.

The measuring devices consisted of the following equipment:

(a) A hypodermic needle stagnation tube, and a 0.120 O.D. stainless steel Pitot tube; (b) A 1.0 psid Statham transducer for measuring the velocity pressure; and (c) An x-y plotter (recorder), for recording the voltage of the pressure transducer output as function of the linear East-West distance along which the velocity distribution was measured; and (d) A water manometer for the measurement of large pressures, especially for high velocities at the orifice. Pressure lines from the Pitot tube were run along the carriage to the scaffold, then down to the floor where they were connected to the transducer.

2.3 Measuring techniques.

Profiles of velocity pressure along a line at the nozzle outlet, from which the efflux velocities and flow rates were figured, were obtained by use of the hypodermic needle stagnation tube, connected directly to the water manometer.

Above the nozzle efflux section, profiles of velocity pressures along a line were taken in an East-West direction, with the East-West position and velocity pressure at each point being recorded on the x-y recorder. The North-South position and elevation were recorded manually.

As the velocities must be sampled in space and in time because of turbulent fluctuations, the proper procedure would have been to select points and directions at which the time-average velocities would be determined. For each of these points and directions a time series of velocity pressure should have been recorded for a sufficiently long time to decrease the sampling error in determining the time-average velocity to a small tolerable magnitude. The time series of Pitot tube velocity pressure then should have been transformed to velocity time series by using the velocity-pressure relationship from the Pitot tube calibration and for the proper density of the fluid at the time of measurement. Also, corrections should have been made for turbulent velocity fluctuations so that the time-average velocity would have been obtained, rather than the momentum flux average velocity. From the velocity time series the time-average velocity would have been determined. All these average velocities for a cross section at the points of measurement and in the given direction would have determined the velocity distributions either along a line or over a plane, usually of the velocities perpendicular to that line or that plane. However, this most ideal measuring technique would have necessitated the spending of an enormous amount of time for data collection and also would have required an elaborated procedure of data processing. This procedure, therefore, was used only in measuring the velocity profile at the efflux section of the jet orifice.

The following measuring technique was applied to the cross sections (planes) perpendicular to the jet-axis and at a distance X from the orifice. Traverses for several different values of Z were made of the relationship, velocity pressure versus the length in the cross section plane. By slowly moving the Pitot tube rider, the velocity pressure profiles along the selected lines in the cross section plane were recorded. Figure 12 shows such a recorded profile. Since the voltage output was linearly related to the Pitot tube pressure, the simple linear transformation of the scale of profile ordinates gave the velocity pressure profile. The velocity pressure thus fluctuated around an average central smooth line which represents the time-average velocity pressure along the traverse line. As figure 12 shows the

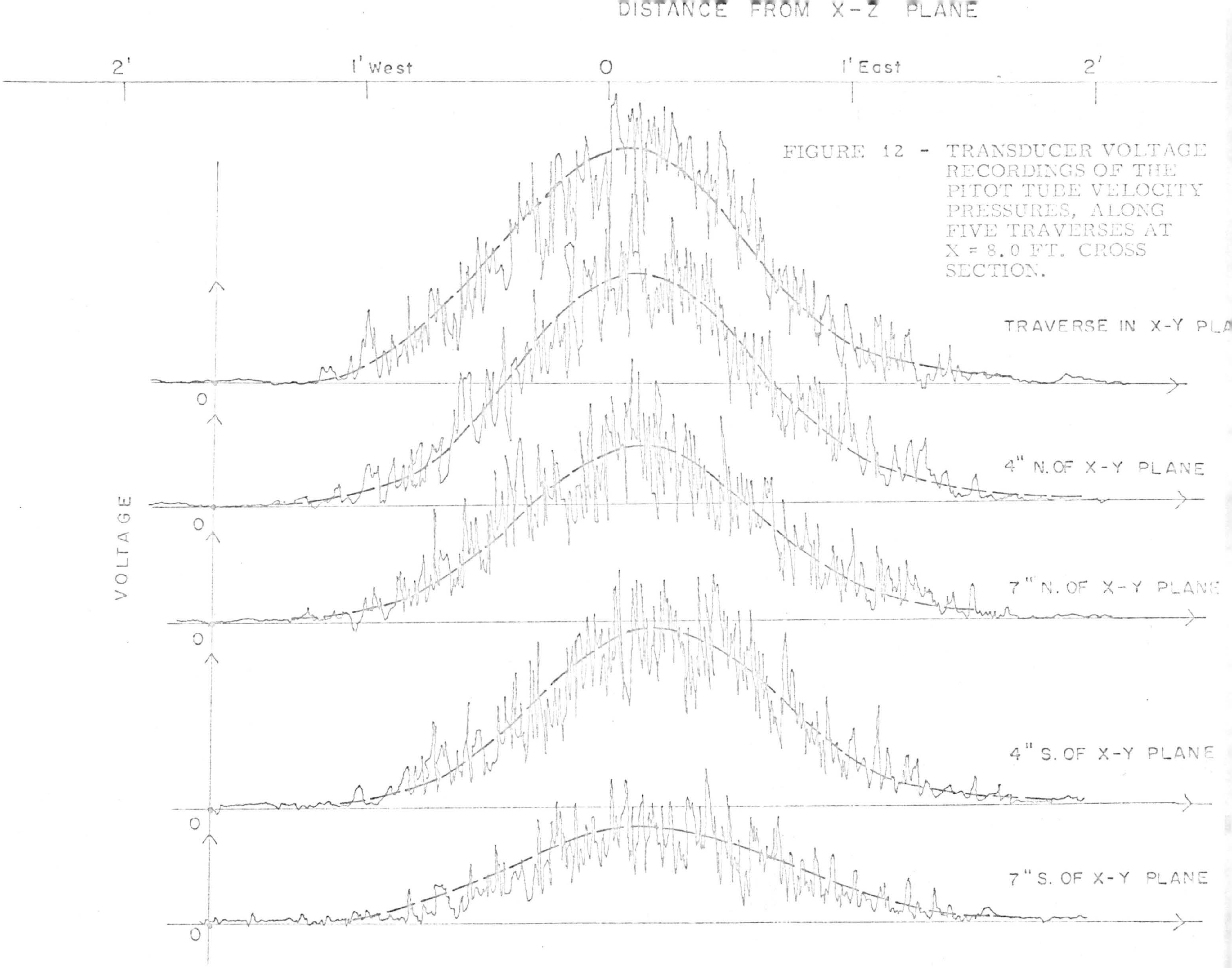

FIGURE 12 - TRANSDUCER VOLTAGE RECORDINGS OF THE PITOT TUBE VELOCITY PRESSURES, ALONG FIVE TRAVERSES AT X = 8.0 FT. CROSS SECTION.

instantaneous velocity pressure is recorded along a traverse line. The neighboring points give different instantaneous pressures, so that an averaging process of this fluctuating velocity pressure produces the approximate distribution of the time-average velocity pressure.

2.4 Experimental procedures and data collection.

Two sets of runs were conducted, a set of runs consisting of experiments with nozzles of the same cross sectional area. These two sets refer to areas of 1.844 square inches and 1.000 square inches respectively. For each set five different length-width ratios L_o/B_o were used, or altogether ten different slots. The eleventh nozzle was the circular one with the area 1.000 square inch.

Three different flow rates were used for each nozzle. They were governed by regulating the area of the blower inlet, and had values of approximately 2.2, 4.2, and 6.5 c.f.s. for nozzles of 1.844 square inch area, and 1.3, 2.3 and 3.7 c.f.s. for the 1.000 square inch area nozzles. The reason for changing the set of flow rates with area was the result of an attempt to keep the nozzle orifice velocities V_o for the various discharges the same in both sets of nozzles. Approximate values of V_o for the three flow rates were 180, 330, and 520 f.p.s. for all eleven nozzles. Flow rates were computed by graphical integration from the velocity pressure profiles taken at the nozzle outlet.

The data taking procedure for each nozzle was as follows: The blower was started and the air temperature at the nozzle exit measured. When the jet air at the efflux reached approximately a temperature of about 98°F, it was held constant by use of the external water bath and water spray over the blower. Wet bulb and dry bulb temperatures of the ambient air were taken at the beginning and end of each run and averaged. Barometer readings were taken from a continuous recorder. The ambient temperature was usually around 85°F.

After the nozzle temperature had stabilized, velocity pressure profiles were taken with the hypodermic stagnation tube at the nozzle outlet and the velocity pressure on the jet-axis was taken with the same stagnation tube a elevations of 1.00 and 1.50 feet above the nozzle. The flow rate was then changed and the same procedure followed for the other two flow rates. Flow rates were set by measuring the velocity pressure at the nozzle cutlet on the central jet-axis.

Velocity pressure profiles above the jet were taken at elevations ranging from 1.4 feet to 14.4 feet, with approximately 5 equal logarithmic intervals starting at the lower elevation. At each elevation except at 14 feet, five velocity pressure line profiles were taken in the East-West direction: one on the East-West plane of symmetry and two on either side of that plane. One to three profiles were taken at the 14 foot elevation depending on the discharge, because velocities at this elevation were quite small. A velocity pressure measurement for each run was also taken on the axis of symmetry at an elevation of 21.75 feet.

The method of recording each velocity pressure profile was to start the Pitot tube measurements outside the measurable flow region at a fixed North-South position and draw the Pitot tube across the flow in an East-West direction at a rate of about one to two feet per minute (recording the velocity pressure and East-West location on the x-y recorder), until it had reached the opposite side of the flow region. After recording the profiles for one flow rate at any elevation, the flow rate was changed and the profiles for the next flow rate were recorded.

When profiles for all three flow rates had been taken, the carriage was moved to the next elevation and the procedure was repeated.

2.5 Data processing.

The digital computer was used in order to minimize the time for data processing. The graph of velocity pressure versus the distance was smoothed by drawing an average line through the fluctuating values, as it is shown in figure 12. Values of voltage from this average line were taken at equal horizontal distances and tabulated. This data was then punched onto data cards, and all computations were carried out by a digital computer.

2.6 Error sources in the data.

There were several factors involved in the experimental equipment and in the data taking technique which could have introduced errors into the observed data. These factors are mentioned below for the benefit of the reader in his evaluation of the reliability of the conclusions derived. No attempt has been made to analyse the exact effect of these factors; however, it is felt that the total effect of these factors introduced no more than a couple percent of the errors in the computed velocities.

2.61 Turbulence generated by the blower. Because the blower was of centrifugal type, the air exiting from the blower necessarily was highly turbulent. The only resemblance of an attempt to straighten the flow was the use of turning vanes in the elbow. Above the vanes was a stilling chamber 14" x 14" and 12" long. The velocities in the elbow section, however, were approximately 1 to 3 f.p.s., which allowed a short period for the air coming from the blower to develop into a uniform flow. The actual condition of turbulence along the path approaching the nozzle and in the nozzle was not investigated.

2.62 Length of nozzles. It is felt that the nozzle lengths (parallel to the flow) used in these experiments were too long. The length of the nozzle permitted a boundary layer to develop. Its effect was noticed by the slight curvature of the velocity profile near the edges of the orifice. In order to direct the jet vertically with the slightest possible deviation from the theoretical axis, it was found that a nozzle of some length was necessary.

2.63 Temperature difference between the jet at the efflux section and the atmosphere. The temperature difference between the flow leaving the orifice and that of the ambient fluid was usually about 15^{0}F. This temperature difference resulted in a buoyancy force directed upwards along the jet-axis. As was staed earlier in this text, the jet outlet velocities were large (180-520 f. p. s.) so that the velocity caused by the buoyant force was very small in comparison with the jet velocities, and the mixing of the hotter jet air and the environmental air progressed fast enough along the jet axis so that at an elevation of 1.5 feet there was less than 1^{0}F difference in temperature between the jet fluid and the ambient fluid.

2.64 Shifting of jet-axis. Regardless of the precautions taken to avoid introduction of external air currents in the laboratory (closing laboratory doors and turning off all heaters in the laboratory), there were some low speed horizontal air currents observed in the laboratory during the experiment. These currents plus the difficulty of fixing the nozzles with their X axis exactly vertical, made the jet expansion such that the point of maximum velocity in the cross sections sometimes deviated slightly from the vertical line through the nozzle center. However, these deviations were relatively small and in the order of about 2 or 3 inches from the vertical axis at an elevation of 15 feet above the nozzle.

2.65 Data taken at elevation of 21.75 feet. The data taken at this elevation consisted only of a measurement of maximum velocity. It was found that these velocities did not fit the general trend of the other data; they were usually somewhat lower than the general trend of data would indicate that they should be. Since there was not sufficient data taken in this region to substantiate a definite change in behavior of the jet and since this point was quite near the ceiling, this data was discarded. It is thought that the cause of the lower velocity may have been the effect of the ceiling boundary which was quite close to this point of measurement (see figure 7). For the free submerged jet it is assumed that the fixed boundaries are at such distances that they do not affect the flow patterns; this condition was not satisfied at the elevation of 21.75 feet.

2.66 Measurement of velocity pressure. The errors in velocity measurement resulted from several causes. First, as mentioned previously under 2.3 "Measuring Techniques", the profiles of instantaneous velocity pressure were taken along the traverses at the cross sections rather than using the time series technique as observed at each point. Second, the instantaneous velocity pressures were measured by voltage output from a pressure transducer. Because the Pitot tube was connected to the pressure transducer by plastic tubes, some attenuation of pressure extremes was produced both by the connecting plastic tubes and by the inertia of transducer diaphragm. This in turn decreased somewhat the standard deviation of the instantaneous velocity pressure around the mean velocity pressure as compared with the true standard deviation at the point. As the time-average velocity is a function of the square root of pressure, $\sqrt{\rho}$, the square root of average pressure $\sqrt{\bar{\rho}}$, is usually greater than the average value of square root of pressure, $\overline{\sqrt{\rho}}$. Thus, the Pitot tube gives somewhat greater velocities when the average pressure is used than when time fluctuating velocity pressure at a point is converted to the velocity and then velocity time series averaged. The greater the standard deviation of velocities around the average velocity, the larger is this overestimate of time-average velocities. Therefore, the attenuation of extreme velocity pressures by measuring technique used and the use of time-averaging of Pitot pressure in computing the time-average velocity both work in the same direction of overestimating the velocities.

The next error comes from the drawing of an average velocity pressure line on the pressure fluctuating along a traverse, as shown in figure 12. The correct procedure for finding the average point velocities from the fluctuating curve of velocity pressure along a traverse would have been to smooth the curve by an averaging procedure, or to draw the upper and lower envelopes of the curve, compute the velocities and then take the average as a better approximation than drawing the average curve as was done in figure 12. However, a check of the error involved between the procedure used and the ideal procedure for finding velocities amounted to about 0.1 to 0.7 percent.

2.67 Effect of Reynolds Number. Since no attempt was made to account for Reynolds number in analyzing the data (or assuming that Reynolds number has a small effect on the jet diffusion for highly turbulent flows), some small errors are inherent because of the effect of Reynolds number on the diffusion process.

3. ANALYSIS OF EXPERIMENTAL RESULTS

3.1 Values computed from processed data.

The procedure for processing the raw data in order to obtain the computed values is as follows. The time-average voltage readings corresponding to the velocity pressures, as represented in figure 12 for several traverses, were punched on computer data cards as discrete values for given Y-values. The Y-values were measured from the traverse center; this center being defined as the point on the traverse straight line, which is the intersection of this line and the X-Z plane as represented in figure 3. The jet air density, for each run, which had been calculated from the measured air temperatures and humidity, was also punched on computer cards. Then the time-average voltages were converted to the velocity pressures and these in turn were converted to the time-average velocities by a digital computer. From these velocities the following magnitudes were computed:

(a) Mean, $\bar{Y}$, of the velocity distribution along the traverse in relation to the traverse center;

(b) Standard deviation, σ, of the velocity distribution about the value $\bar{Y}$;

(c) Maximum velocity, V_m, which would be at the $\bar{Y}$ if the velocity distribution was normally distributed with the above computed standard deviation, σ;

(d) Volume flux per one foot of width Z, normal to the traverse;

(e) Momentum flux per one foot of width Z, normal to the traverse; and,

(f) Energy flux per one foot of width Z, normal to the traverse.

These computed parameters and magnitudes were used in the derivation of other values and of the main relationships to be shown later. For the maximum time-average velocity along the jet-axis, there were two values available: (a) The maximum measured value on the velocity distribution curve (the velocity corresponding to the maximum voltage or velocity pressure on the curve of voltage or velocity pressure distribution, as shown by dashed lines in figure 12); and, (b) The maximum velocity at $\bar{Y}$, computed by the above described procedure. As these two cases will be pursued further in the text as two parallel analyses, whose results will be averaged, they will be called briefly: V_m directly determined, and V_m computed, respectively. The purpose for the use of the computed value V_m is a comparison with the value directly determined which is considered as having a larger subjective error. This error is produced by the method of drawing the time-average velocity pressure, as shown in figure 12, for which it is difficult to avoid some subjectivity, while the computed value V_m has reduced this subjective error to a minimum. However, this computed velocity is subjected to another type of error which is due to the fitting of a normal function to the time-average velocity distributions.

3.2 <u>Comparison of maximal time-average velocities along the jet-axis from this study with previous studies, for the circular and the square orifice jets.</u>

Figure 13 is a comparison of experimental results for circular jets between those of the Iowa Study, line (1), and those obtained in this study, line (2) as fitted to the points designated by symbols 1, 2, and 3. The line (2) coincides with the line (1). Except for the two points at the highest flow rate with V_o = 522 f.p.s. for

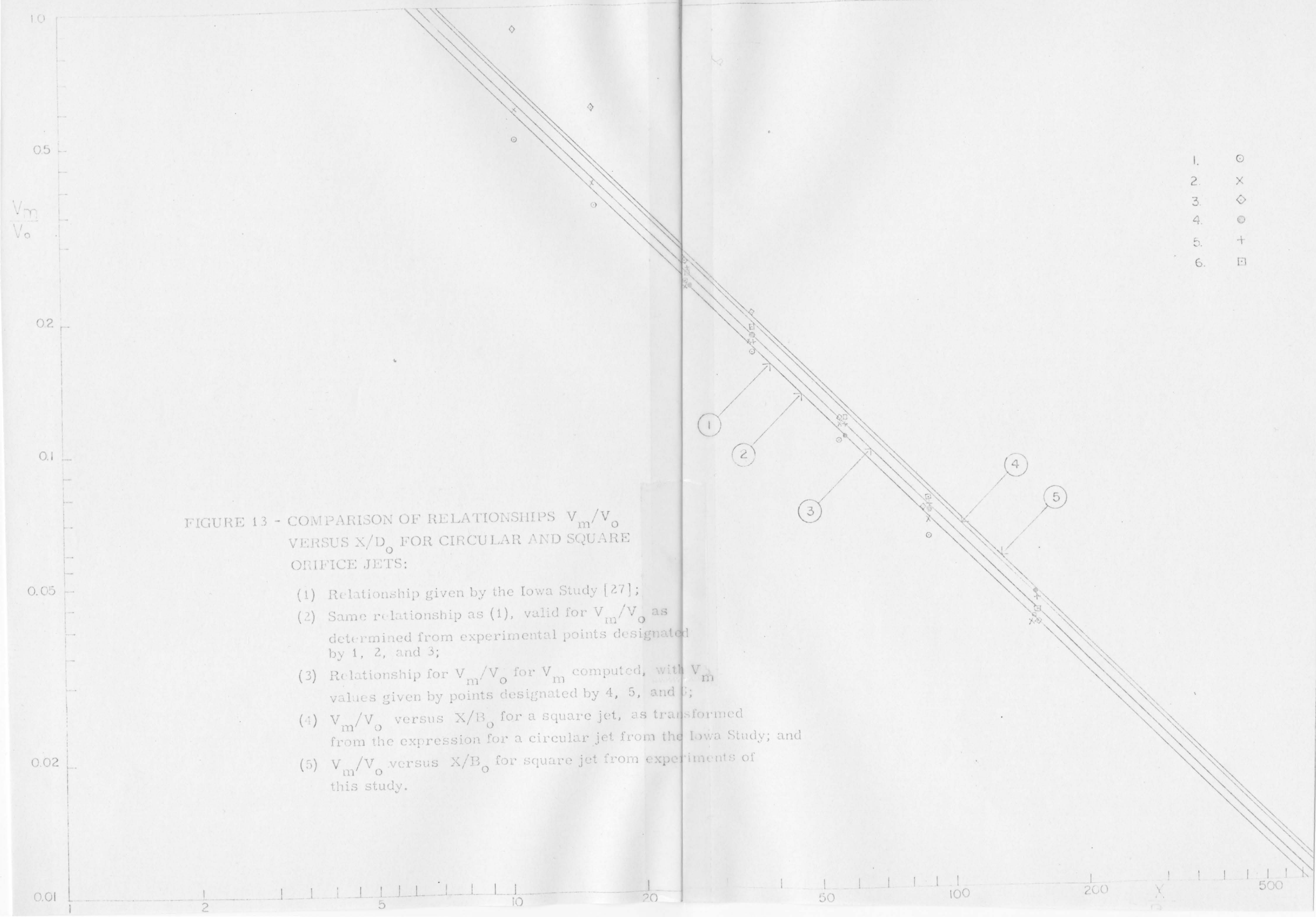

FIGURE 13 - COMPARISON OF RELATIONSHIPS V_m/V_o VERSUS X/D_o FOR CIRCULAR AND SQUARE ORIFICE JETS:

(1) Relationship given by the Iowa Study [27];

(2) Same relationship as (1), valid for V_m/V_o as determined from experimental points designated by 1, 2, and 3;

(3) Relationship for V_m/V_o for V_m computed, with V_m values given by points designated by 4, 5, and 6;

(4) V_m/V_o versus X/B_o for a square jet, as transformed from the expression for a circular jet from the Iowa Study; and

(5) V_m/V_o versus X/B_o for square jet from experiments of this study.

$X/D_o = 10.7$ and $X/D_o = 16$, all other points, with V_m determined directly, fluctuate well around the line (1) given by the Iowa Study, wi h $V_m/V_o = 6.2\ D_o/X$. These two points with a large deviation from the line may be the result either of a large Reynolds number, $R_e = 2.12 \times 10^5$ (this number is defined by using D_o as the geometric characteristic of the orifice instead of using the hydraulic radius $R = D_o/4$), or the points may be in error because of the measuring technique used (the use of the hypodermic needle in a highly turbulent flow of blower type air supply).

Table 1 gives the Reynolds numbers for all experimental runs of the 11 different nozzles which include three different flow rates for each nozzle, altogether 33 experiments. The Reynolds numbers are given for two different characteristics lengths of orifice: (a) Hydraulic radius with $R = D_o/4$ for circular orifice, and $R = L_o B_o/2(L_o + B_o)$ for the slot orifices; and (b) D_o or B_o as the characteristic length. In the first case, R_e fluctuates from $R_e \cong 0.4 \times 10^4$ to $R_e \cong 6.6 \times 10^4$, while in the second case it fluctuates from $R_e \cong 0.8 \times 10^4$ to $R_e \cong 2.6 \times 10^5$. Assuming that Baines [27] had used the second definition of Reynolds number (with D_o or B_o as the characteristic length), and by using his empirical relationship of X_o/D_o versus R_e [27, fig. 26], then for $R_e = 0.8 \times 10^4 - 2.6 \times 10^5$ and for the blower type of air supply, X_o/D_o should fluctuate somewhere between 5.0 and 6.0. The experimental points for three flow rates, with $V_o = 180$, 329, and 522 f. p. s., respectively, show that there is an effect of the Reynolds number, indicating that for $R_e = 7.34 \times 10^4$ the value X_o/D_o may be somewhat smaller than for the value $R_e = 21.2 \times 10^4$. However, the precision of experimenta points in both Baines data and in the results of this study is not such as to enable a clear discrimination of the way in which X_o/D_o changes with a change of Reynolds number.

The fitting of a straight line (line in fig. 13) of log V_m/V_o versus log X/D_o to the experimental points of V_m/V_o for V_m determined directly, except to the two extremely high points at $X/D_o = 10.7$ and $X/D_o = 16$, shows no practical difference between the Iowa Study, with $X_o/D_o = 6.2$, and this study. However, a fitting of the same relation to the points of V_m/V_o for V_m calculated, (line 3 in fig. 13) shows a straight line which has a somewhat higher position on the graph then that of the Iowa Study. The value X_o/D_o is here 6.55 as opposed to 6.2 for the previous case. The points of V_m/V_o for the computed V_m are designated by symbols 4, 5, and 6.

The relationship of V_m as determined directly versus V_m computed is represented in figure 14. A straight line of 45^0 is plotted with two straight lines around it. These two lines define the envelope of the deviations of velocities from the 45^0 line within $\pm$ 5 percent. The points plotted show that the computed velocities V_m are close to those determined directly for V_m greater than 35 f. p. s., with the spread of points mostly confined within the $\pm$ 5 percent deviation from the 45^0 straight line. For smaller values of V_m, in the range 5-35 f. p. s., there is a general tendency for V_m computed to be somewhat greater than V_m determined directly. Because the relative turbulent fluctuation about the time-average velocity is greater for small values of V_m (see fig. 12), the simple fitting of the time-average velocity pressure line through the recorded velocity pressures along traverses (like the dashed lines shown in fig. 12) may be partly responsible for

TABLE 1

Reynolds numbers for 33 experiments with slot jets and circular jets

L_o in.	B_o in.	Hydra Radius ft.	V_o f. p. s.	$R_e = \frac{VR\rho}{\mu}$ * in 10^4	$R_e = \frac{VB_o\rho}{\mu}$ in 10^4
1.340	1.360	0.0282	171	2.13	8.55
			326	4.06	16.3
			532	6.62	26.2
3.005	0.610	0.0212	183	1.71	4.10
			338	3.16	7.57
			533	4.98	11.9
5.005	0.370	0.0143	179	1.13	2.43
			335	2.11	4.54
			534	3.43	7.25
7.510	0.245	0.00991	183	0.800	1.64
			336	1.47	3.01
			542	2.37	4.86
10.010	0.185	0.00763	183	0.617	1.25
			332	1.12	2.26
			530	1.78	3.60
0.995	0.995	0.0206	183	1.67	6.74
			330	3.02	12.1
			524	4.79	19.3
2.000	0.500	0.0167	184	1.35	3.36
			332	2.43	6.07
			527	3.86	9.64
4.000	0.250	0.00983	179	0.781	1.66
			326	1.42	3.02
			511	2.23	4.73
7.012	0.153	0.00625	184	0.508	1.04
			336	0.928	1.89
			514	1.42	2.89
9.870	0.105	0.00433	205	0.396	0.800
			353	0.683	1.38
			494	0.955	1.93
1.125 (D_o)	circular	0.0234	180	1.91	7.34
			329	3.48	13.4
			522	5.53	21.2

* Air density ρ in 10^3 lbs. sec^2/ft^4 was approximately in the limits 1.78 to 1.83. Viscosity μ in 10^7 lbs. sec/ft^2 is 4.1.

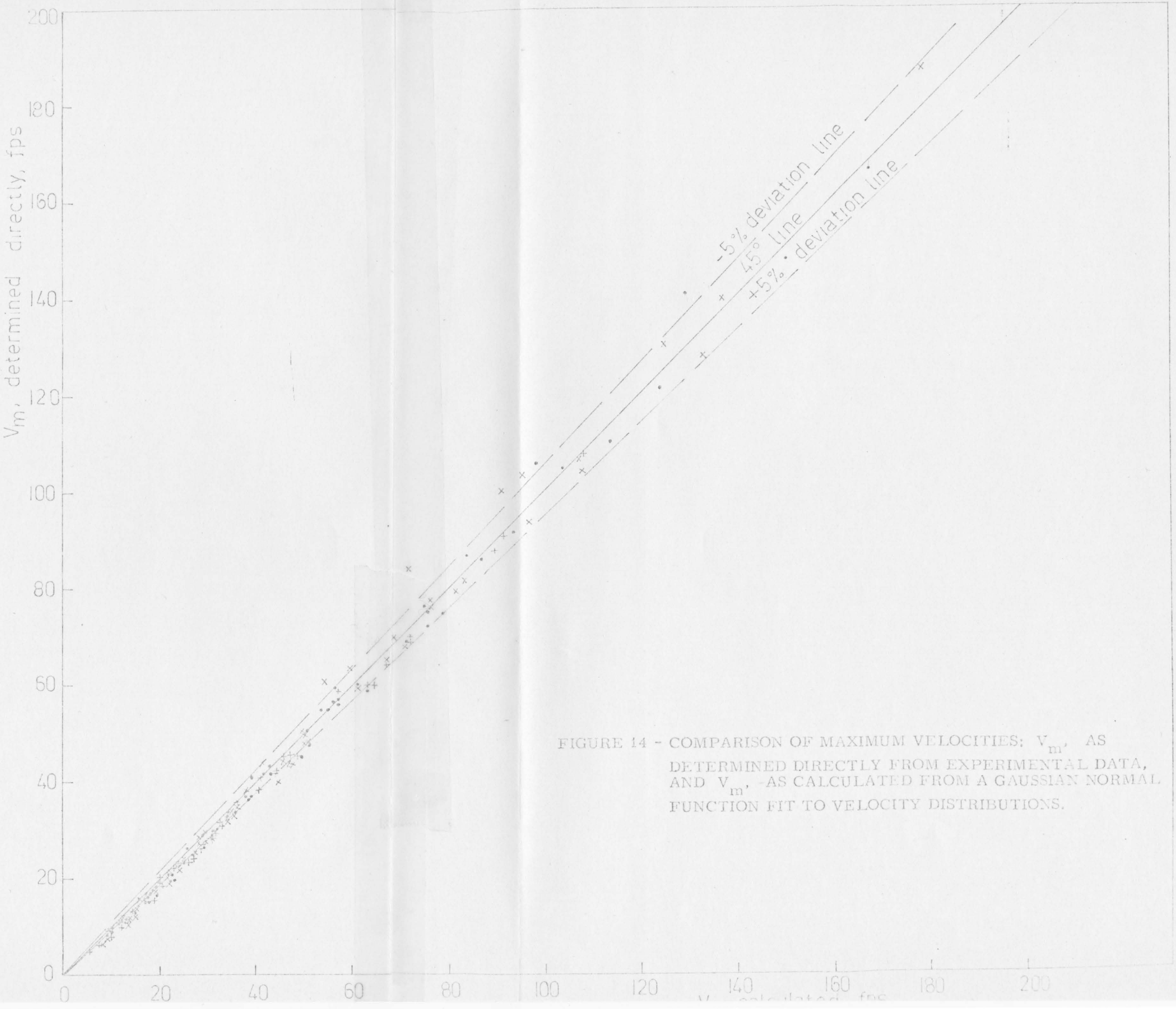

FIGURE 14 - COMPARISON OF MAXIMUM VELOCITIES: V_m, AS DETERMINED DIRECTLY FROM EXPERIMENTAL DATA, AND V_m', AS CALCULATED FROM A GAUSSIAN NORMAL FUNCTION FIT TO VELOCITY DISTRIBUTIONS.

these differences in V_m in the range 5-35 f. p. s. This comparison of V_m-values, computed and determined directly, shows that the difference is small, and that both values for V_m may be considered as sufficiently accurate for practical purposes. The further analysis of experimental results will, therefore, be based on both methods of obtaining V_m, with an averaging procedure used for the final results.

Figure 13 shows also the comparison between the square orifice jets among themselves and with circular jets. The line (4) gives the square jet relationship of log V_m/V_o versus log X/B_o, which is a transformed equation from the relationship of the Iowa Study for circular jets, by the relationship $D_o = 1.128\ B_o$, with $V_m/V_o = 7.0\ B_o/X$. The experimental points in this study for V_m/V_o versus X/B_o of square jets produced the line (5) in figure 13 by the least square fit of a straight line. Two different orifice areas B_o^2 were used, and the experiments had three different flow rates for each of them, altogether 6 experiments. The value X_o/B_o, obtained by transforming the value $X_o/D_o = 6.2$ for a circular orifice from the Iowa Study to X_o/B_o for a square orifice is 7.00, while this study produced $X_o/B_o = 7.2$. Taking into account the differences in Reynolds numbers between the two studies, as well as the inherent measuring and computational errors in both studies, the agreement seems satisfactory.

3.3 Deceleration of slot jets for various orifice length-width ratios.

The deceleration of slot jets of various orifice length-width ratios was analyzed by the relationship V_m/V_o versus X/B_o, for both the velocity V_m determined directly, and the velocity V_m calculated. Figure 15 represents a general plot of all experimental

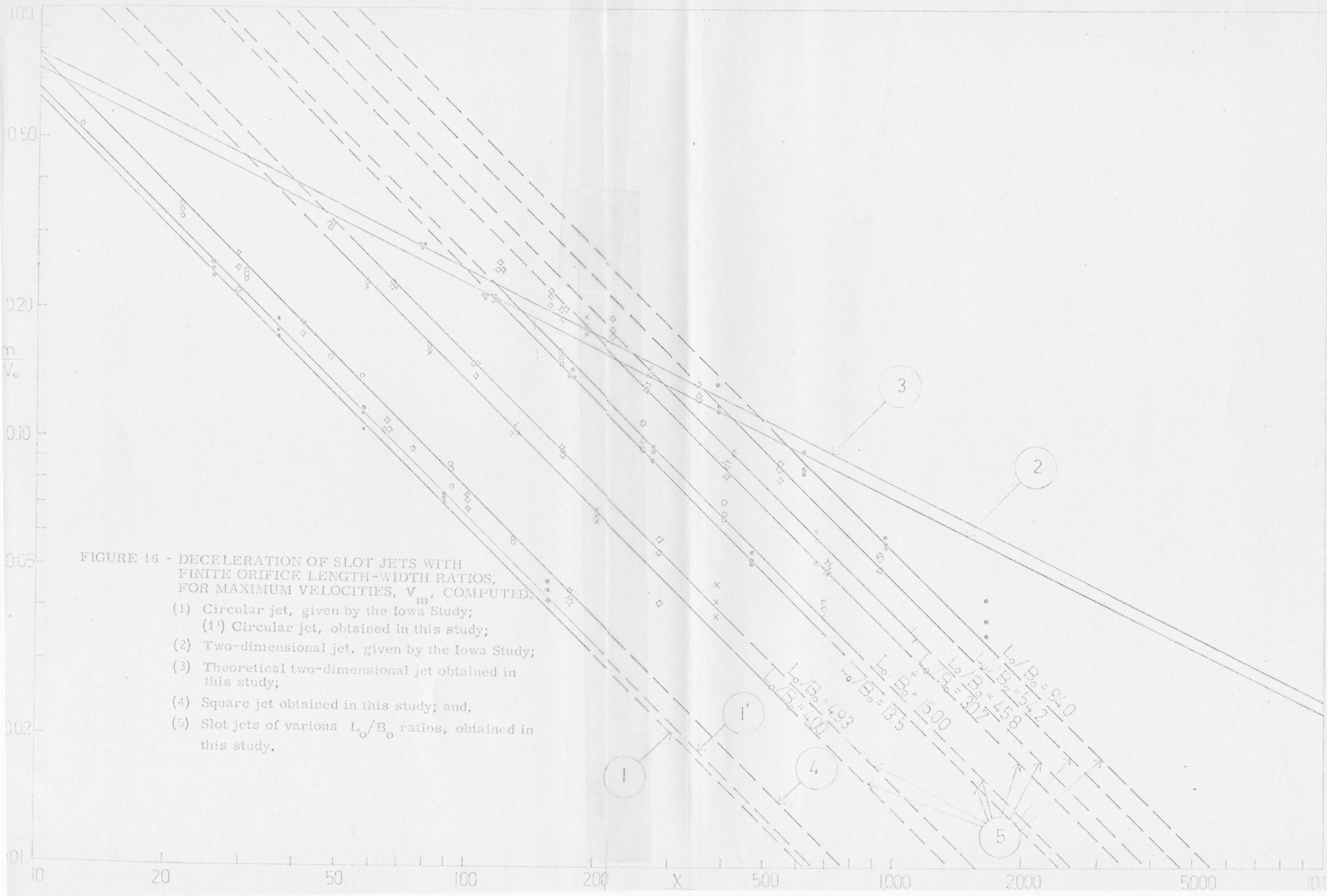

FIGURE 16 - DECELERATION OF SLOT JETS WITH FINITE ORIFICE LENGTH-WIDTH RATIOS, FOR MAXIMUM VELOCITIES, V_m, COMPUTED.

(1) Circular jet, given by the Iowa Study;
 (1') Circular jet, obtained in this study;
(2) Two-dimensional jet, given by the Iowa Study;
(3) Theoretical two-dimensional jet obtained in this study;
(4) Square jet obtained in this study; and,
(5) Slot jets of various L_o/B_o ratios, obtained in this study.

data available for V_m/V_o versus X/B_o from this study for V_m directly determined. The bottom left points refer to the circular orifice and represent, therefore, the relationship V_m/V_o versus X/D_o, while all other relationships are V_m/V_o versus X/B_o. The deceleration for the circular jet and the two-dimensional slot jet of infinite length-width ratio as given by the Iowa Study are the lines (1) and (2) of figure 15, respectively.

For each of the ten slot jets with finite slot length-width ratios (two of them being square slot jets with $L_o/B_o = 1$), a straight line, having a slope equal to that of the line defining the deceleration of the circular and square jet, was fitted to the experimental points lying below the line describing the infinite two-dimensional jet in the Iowa Study. The intercept of each of these lines with the ordinate, $V_m/V_o = 1.00$, was determined by applying the method of least squares to the points defining the straight lines mentioned above. The length-width ratios varied from 1 to 94, which was found to cover a sufficient range for the slot jet investigation. Nine lines resulted, and their intersections with the line $V_m/V_o = 1$ are defined as X_1/B_o. Their intersections with the line of the two-dimensional jet (lines 2 and 3 in fig. 15) are defined as X_2/B_o. Since the intersections of parallel straight lines with the two fixed straight lines are uniquely related, the values X_1/B_o and X_2/B_o are also uniquely related.

Figure 16 shows the same relationship as figure 15, except that figure 16 relates to the V_m/V_o ratios determined from the calculated V_m velocities. Values of X_1/B_o and X_2/B_o for both cases of V_m, V_m determined directly and V_m calculated, are given in Table 2.

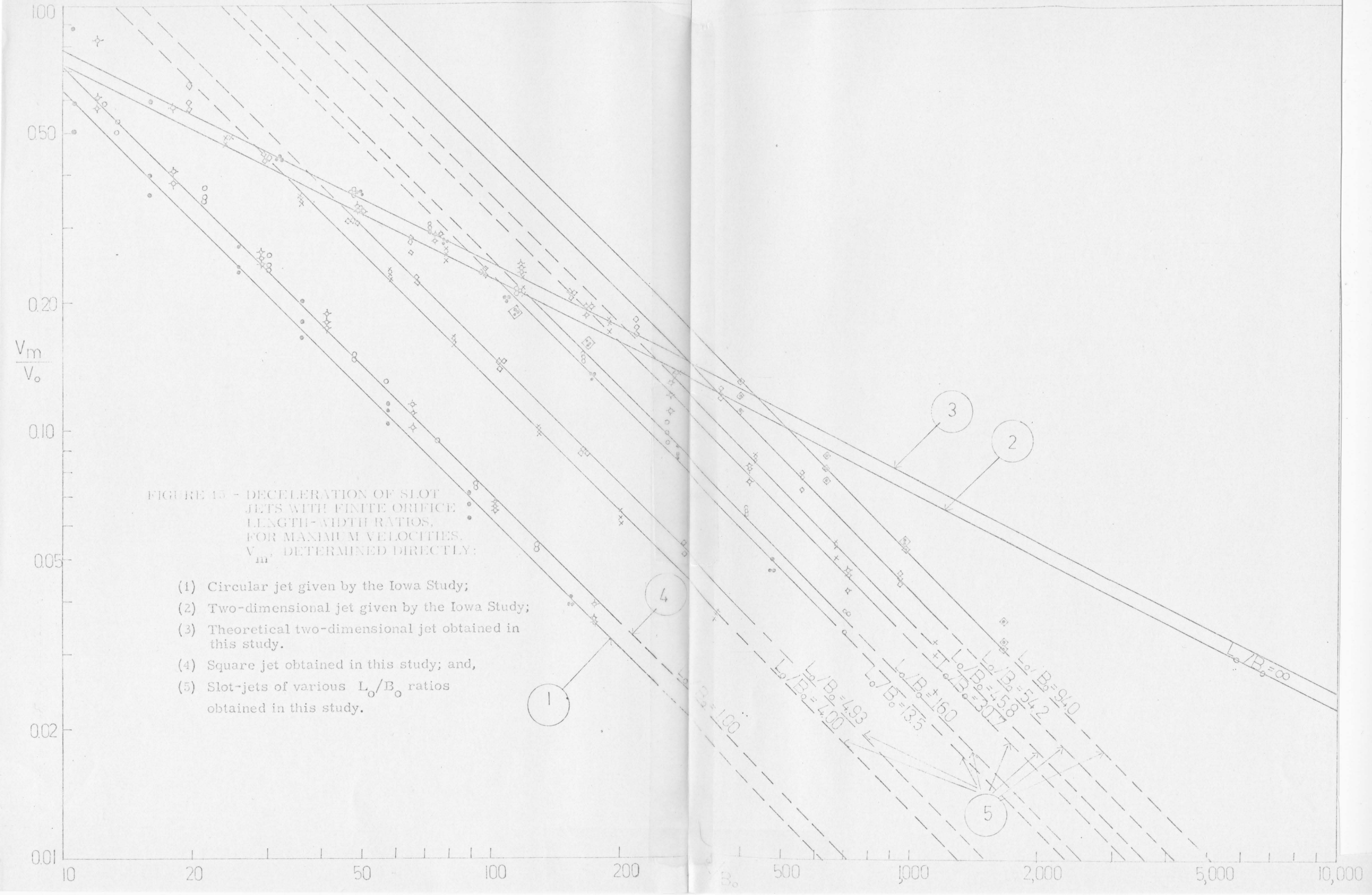

FIGURE 15 - DECELERATION OF SLOT JETS WITH FINITE ORIFICE LENGTH-WIDTH RATIOS, FOR MAXIMUM VELOCITIES, V_m, DETERMINED DIRECTLY:

(1) Circular jet given by the Iowa Study;

(2) Two-dimensional jet given by the Iowa Study;

(3) Theoretical two-dimensional jet obtained in this study.

(4) Square jet obtained in this study; and,

(5) Slot-jets of various L_o/B_o ratios obtained in this study.

The general patterns, as detectable from figures 15 and 16, are that the experimental points V_m/V_o versus X/B_o follow approximately the line of the two-dimensional slot jet of $L_o/B_o = \infty$ for values of X/B_o up to a value $X/B_o = X_2/B_o$, which depends on L_o/B_o. For larger values X/B_o beyond X_2/B_o the experimental points follow approximately the straight lines in graphs with the log-log scales, which lines are parallel to the slope of circular or square jets. It should be stressed, however, that the V_m values refer to the center maximum velocities on the jet-axis at distances X/B_o from the orifice.

Figure 17 shows only the points V_m/V_o versus X/B_o (using V_m directly determined) for the slot jets where $X/B_o < X_2/B_o$ for each L_o/B_o ratio. Most of these points are somewhat above the line of the two-dimensional jet given by the Iowa Study, but the deviations are relatively small. A least squares fit to the points in figure 17 for a straight line parallel to the line of the Iowa Study gives

$$\frac{V_m}{V_o} \quad \frac{X}{B_o} = 2.42 \qquad (14)$$

which is similar to equation (1) of the Iowa Study where the constant is 2.28 instead of 2.42.

Equation (14) is based on V_m directly determined. The constant on the right side of equation (14) would be somewhat greater for V_m calculated.

The relationship of X_1/B_o and X_2/B_o is obtained from equations (1) and (3), by using equation (3) with various positions X_1/B_o, and equation (1) as the line for the two-dimensional jet. The

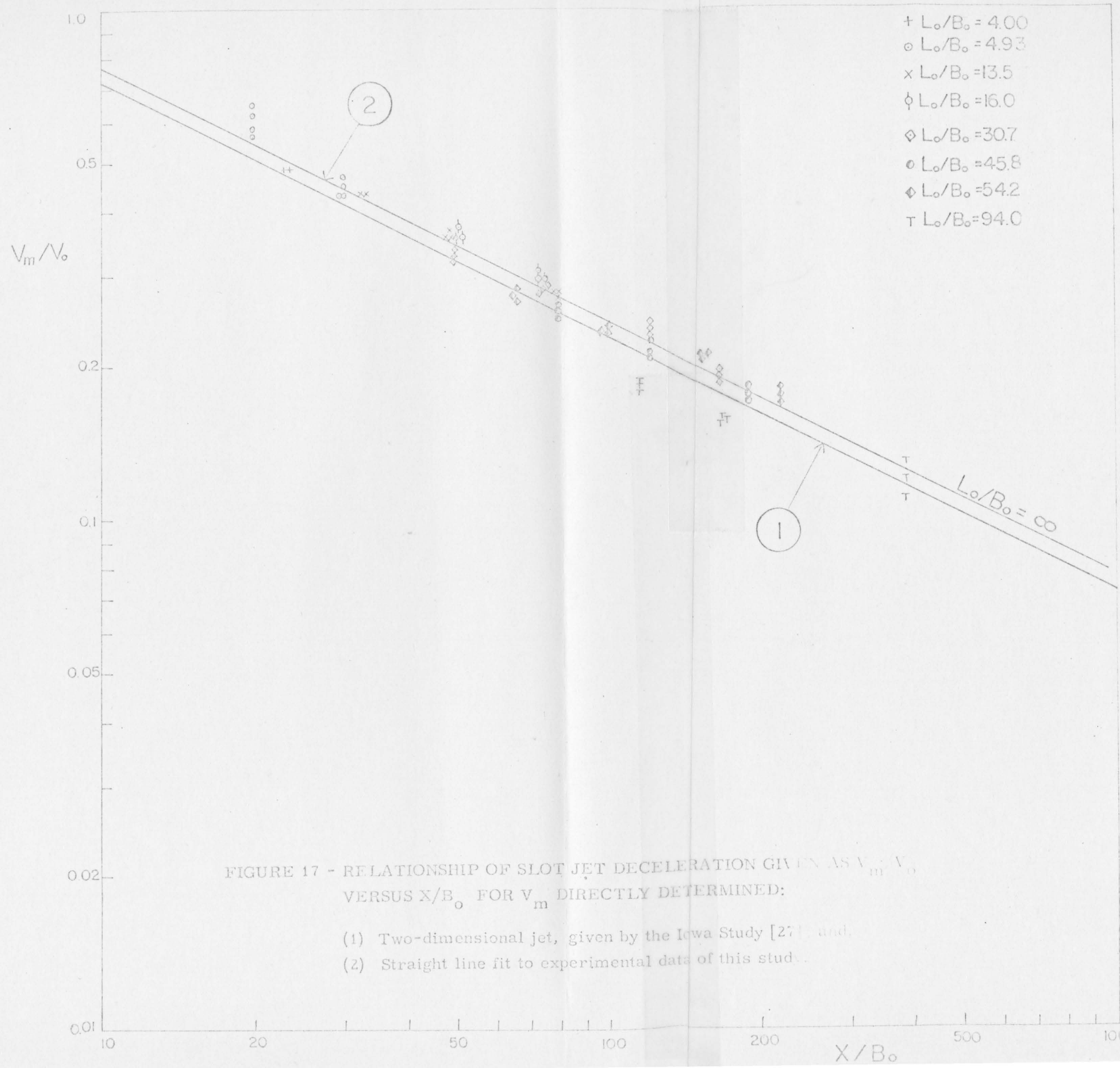

FIGURE 17 - RELATIONSHIP OF SLOT JET DECELERATION GIVEN AS V_m/V_o VERSUS X/B_o FOR V_m DIRECTLY DETERMINED:

(1) Two-dimensional jet, given by the Iowa Study [27] and

(2) Straight line fit to experimental data of this study.

TABLE 2

VALUES OF X_1/B_o AND X_2/B_o

	For V_m determined directly			For V_m computed		
L_o/B_o	X_1/B_o	X_2/B_o*	X_2/B_o**	X_1/B_o	X_2/B_o*	X_2/B_o**
Circular orifice	6.20	7.404	6.57	6.53	8.19	7.27
1.00	7.11	9.725	8.63	7.69	11.37	10.10
4.00	13.07	32.87	29.19	13.6	35.67	31.67
4.93	15.06	43.61	38.73	15.5	46.36	41.17
13.5	23.20	103.7	92.09	24.6	117.0	103.9
16.0	25.30	123.1	109.3	26.3	133.1	118.2
30.7	32.25	201.0	178.5	34.6	230.3	204.5
45.8	35.82	246.9	219.2	38.6	286.5	254.4
54.2	42.66	350.1	310.9	46.3	411.4	365.3
94.0	51.17	503.7	447.3	54.5	570.4	506.5

* Intersection with two-dimensional jet in the Iowa Study.

** Intersection with theoretical two-dimensional jet of this study.

lines for various L_o/B_o ratios, parallel to the line of the square jet, are

$$\frac{V_m}{V_o} \quad \frac{X}{B_o} = \frac{X_1}{B_o} \tag{15}$$

and the two-dimensional jet line is

$$\frac{V_m}{V_o} \sqrt{\frac{X}{B_o}} = b \tag{16}$$

with $b = 2.28$ from the Iowa Study, or $b = 2.42$ from equation (14).

The intersection X_2/B_o of the slot jet lines, equation (15), and the line of equation (16) is

$$\frac{X_2}{B_o} = \left(\frac{X_1}{b\ B_o} \right)^2 \tag{17}$$

Figure 18 gives the relationship of X_1/B_o versus L_o/B_o, fitted by the least squares method. For V_m determined directly, (fig. 15)

$$\frac{X_1}{B_o} = 7.32 \left(\frac{L_o}{B_o} \right)^{0.433} \tag{18}$$

and for V_m calculated (fig. 16)

$$\frac{X_1}{B_o} = 7.68 \left(\frac{L_o}{B_o} \right)^{0.437} . \tag{19}$$

These two equations represent, therefore, the points X_1/B_o along the line $V_m/V_o = 1$ for various values L_o/B_o. An average re-

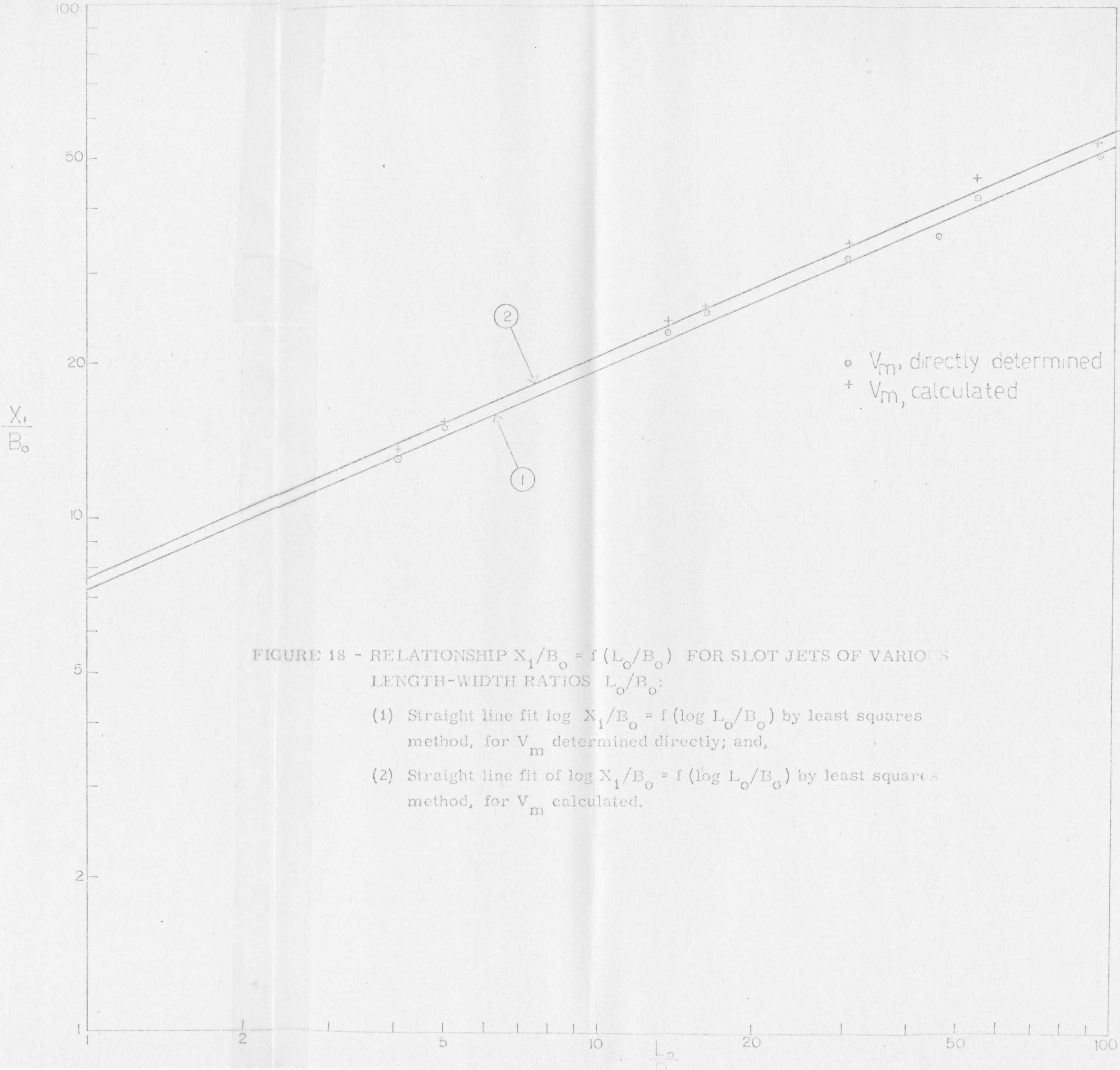

FIGURE 18 - RELATIONSHIP $X_1/B_o = f(L_o/B_o)$ FOR SLOT JETS OF VARIOUS LENGTH-WIDTH RATIOS L_o/B_o:

(1) Straight line fit $\log X_1/B_o = f(\log L_o/B_o)$ by least squares method, for V_m determined directly; and,

(2) Straight line fit of $\log X_1/B_o = f(\log L_o/B_o)$ by least squares method, for V_m calculated.

lationship from equations (18) and (19) is

$$\frac{X_1}{B_o} = 7.5 \left(\frac{L_o}{B_o} \right)^{0.435} . \tag{20}$$

For $L_o/B_o = 1$, $X_1/B_o = 7.5$, which is somewhat greater than 7.2 determined in this study, or 7.0 in the Iowa Study.

To compute X_2/B_o from equation (20), the expressions become

$$\frac{X_2}{B_o} = 10.82 \left(\frac{L_o}{B_o} \right)^{0.87} \tag{21}$$

for $b = 2.28$ of the Iowa Study, and

$$\frac{X_2}{B_o} = 9.605 \left(\frac{L_o}{B_o} \right)^{0.87} \tag{22}$$

from the data of this study.

A direct plot of X_2/B_o versus L_o/B_o and a fit of a straight line in log-log scales, for both V_m directly determined and V_m computed, with an average relationship between the two, shows equations (21) and (22) to be well determined from X_1/B_o and the corresponding b value. Figure 19 is a plot of equations (21) and (22), for a comparison with $X_2/B_o = L_o X_o/B_o^2$, the value of X_2/B_o schematically represented in figure 3. Therefore, for slot jets with a given L_o/B_o ratio, the deceleration of the jet, as measured through the decrease of V_m/V_o versus X/B_o, is

FIGURE 19 - RELATIONSHIP OF X_2/B_o VERSUS L_o/B_o:

(1) Determined from eq. (21), as given by the Iowa Study;

(2) Determined from eq. (22), as given by data from this study;

(3) $X_2/B_o = \frac{X_o}{B_o} \frac{L_o}{B_o}$; for $\frac{X_o}{B_o} = 5.2$ obtained in the Iowa Study;

(4) $X_2/B_o = \frac{X_o}{B_o} \frac{L_o}{B_o}$; for $\frac{X_o}{B_o} = 5.8$ obtained from data of this study.

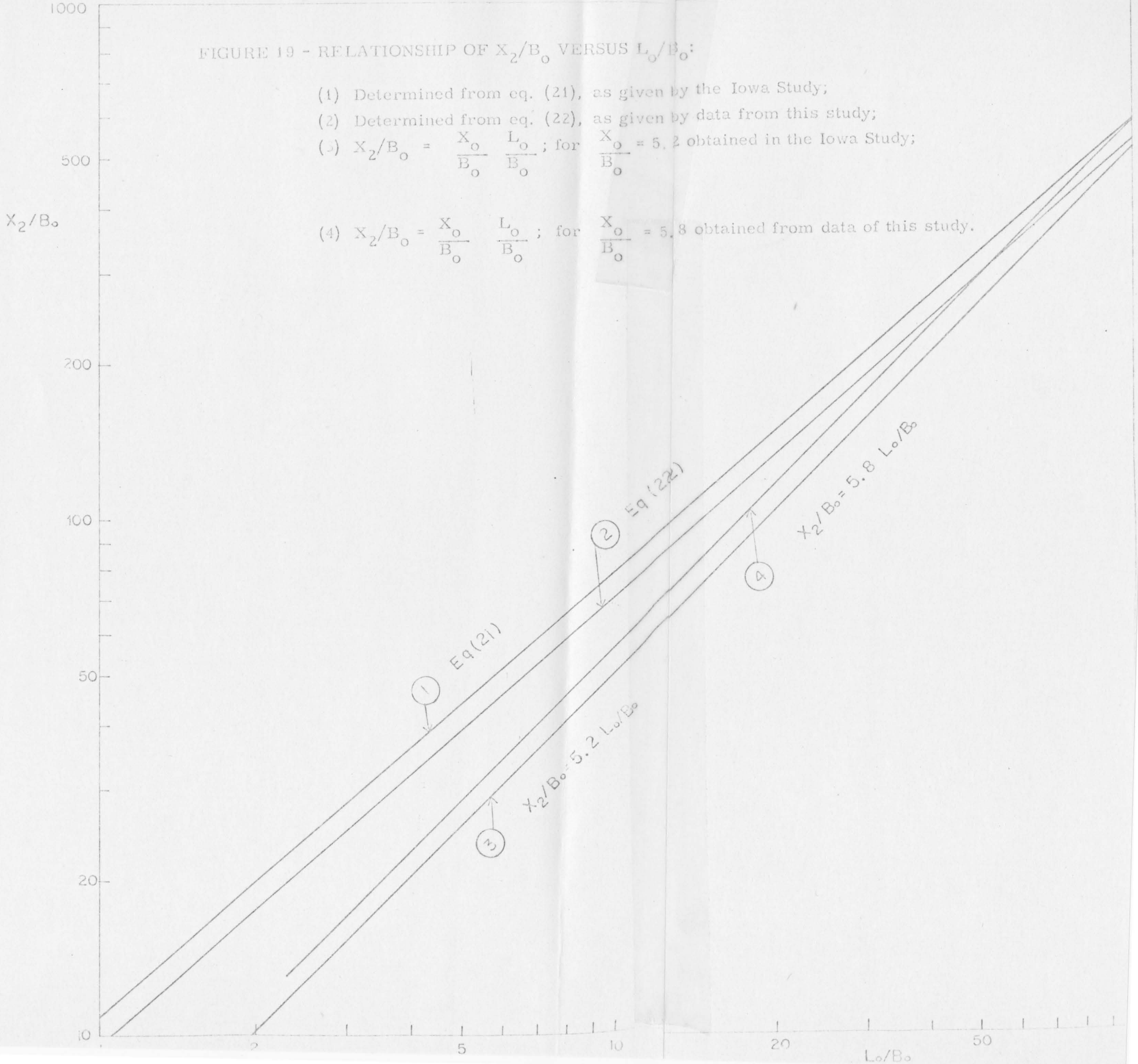

$$\frac{V_m}{V_o} = 1, \tag{23}$$

for $X/B_o \leq X_o/B_o = 5.8$,

$$\frac{V_m}{V_o} \sqrt{\frac{X}{B_o}} = 2.42, \tag{24}$$

for $5.8 \leq X/B_o \leq X_2/B_o$; and,

$$\frac{V_m}{V_o} \frac{X}{B_o} = \frac{X_1}{B_o} = 7.5 \left(\frac{L_o}{B_o} \right)^{0.435} \tag{25}$$

for $X/B_o \geq X_2/B_o$ where X_2/B_o is given by equation (22). In the last two expressions, equations (24) and (25), the values of X_1/B_o and X_2/B_o have been taken as the average values between these given for the two methods of determining the maximum velocity V_m.

The last three expressions, equations (23), (24), and (25), can be used to approximately determine the decrease of the maximum velocity along any slot jet-axis as a function of the L_o/B_o ratio. However, for a first approximation, the value of X_2/B_o may be determined by using the expression $X_2/B_o = X_o L_o/B_o^2$ and the above equations (23) through (25).

Figure 20, based on equations (23) through (25) for V_m/V_o, and on equation (22) for X_2/B_o, represents final results of this study as it relates to the deceleration of the maximum velocity along the slot jet-axis.

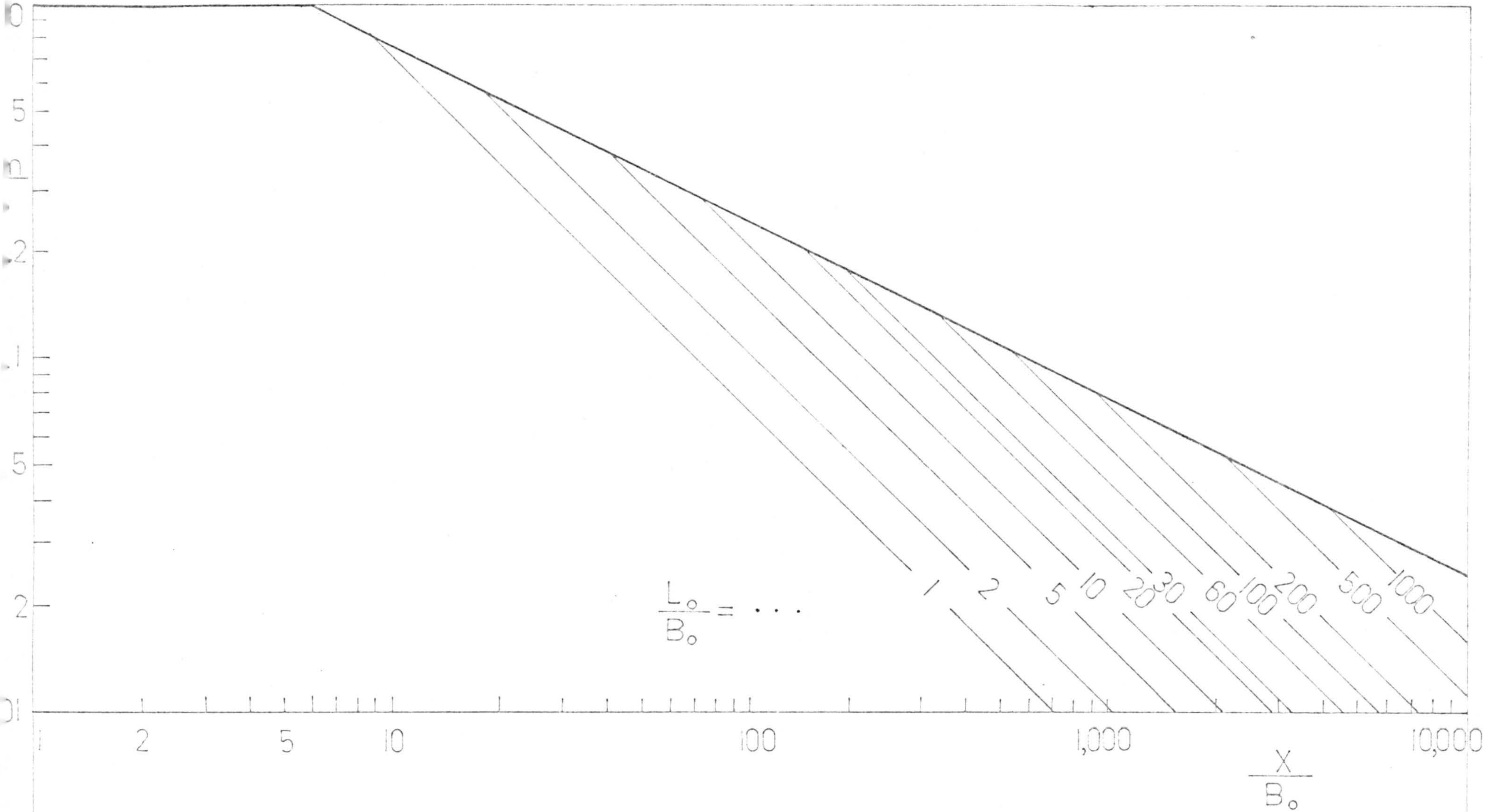

FIGURE 20 - RELATIONSHIP OF V_m/V_o VERSUS X/B_o FOR SLOT JETS OF VARIOUS L_o/B_o RATIOS, AS DETERMINED BY EQUATIONS (22), (23), (24) and (25).

3.4 Deceleration of slot jets of various length-width ratios but with the same orifice area.

Figures 21 and 22 give relationships V_m/V_o versus X in feet of the two series of five nozzles, each series with a constant area $A_o = L_o B_o$, or $A_o = 1.84$ and 1.00 sq. in., respectively. The slot orifices varied from $L_o/B_o = 1$ to 54.2 for the first series, and $L_o/B_o = 1$ to 94.0 for the second sèries, plus the circular orifice jet for the second series.

Taking V_o for each of the five slot nozzles of a series as a constant, which means the same flow rate Q through all nozzles, then figures 21 and 22 represent a comparison of penetration or deceleration of slot jets with various length-width ratios keeping the slot area equal. The results show that the initial V_m/V_o values are smaller for slot jets of high L_o/B_o values than for the square jet or circular jet.

Both regions of slot deceleration as given by equations (24) and (25) are analyzed and compared here for two slot jets: (a) square jet with $L_o/B_o = 1$, and (b) a hypothetical slot jet with $L_o/B_o = a$, for "a" sufficiently larger value than unity. As $L_o B_o = A_o$, then in the square jet $L_o = B_o = \sqrt{A_o}$, and for the slot jet $B_o = \sqrt{A_o/a}$, and $L_o = \sqrt{aA_o}$. Equation (24) is valid for the slot jet for all values of X between X_o and X_2, with $X_o = 5.8 \sqrt{A_o/a}$ with X_2 determined from equation (22) as $X_2 = 9.605 \; a^{0.37} \sqrt{A_o}$. In the range X_o to X_2, the square jet has $V_m/V_o = 7.5 \sqrt{A_o}/X$, and for $V_m/V_o = v$, the square jet has $X_3 = 7.5 \sqrt{A_o}/v$. Equation (24) gives for the slot jet with $L_o/B_o = a$ the value $X_4 = \dfrac{5.85}{v^2} \sqrt{\dfrac{A_o}{a}}$. The difference $\Delta X = X_3 - X_4$ becomes

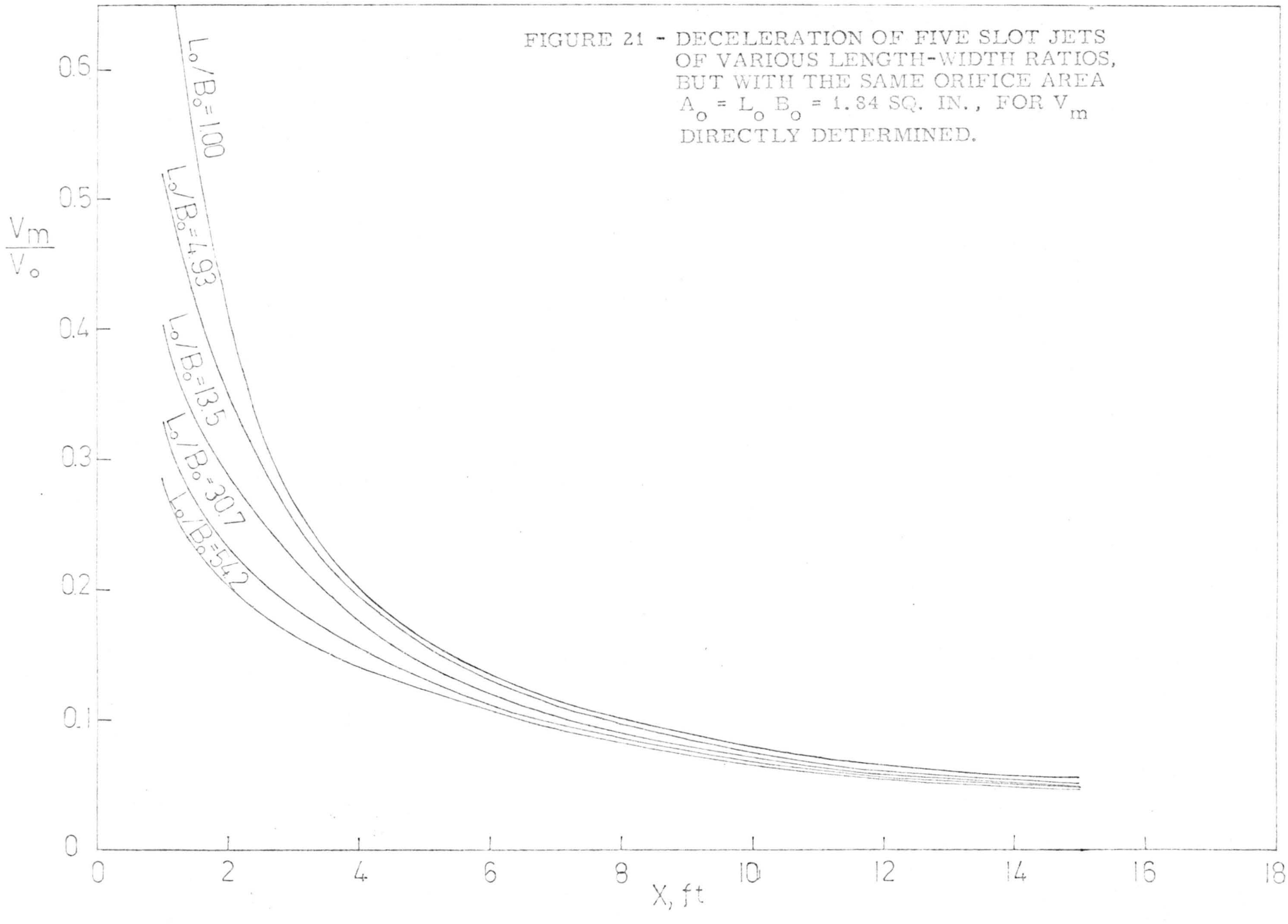

FIGURE 21 - DECELERATION OF FIVE SLOT JETS OF VARIOUS LENGTH-WIDTH RATIOS, BUT WITH THE SAME ORIFICE AREA $A_o = L_o B_o = 1.84$ SQ. IN., FOR V_m DIRECTLY DETERMINED.

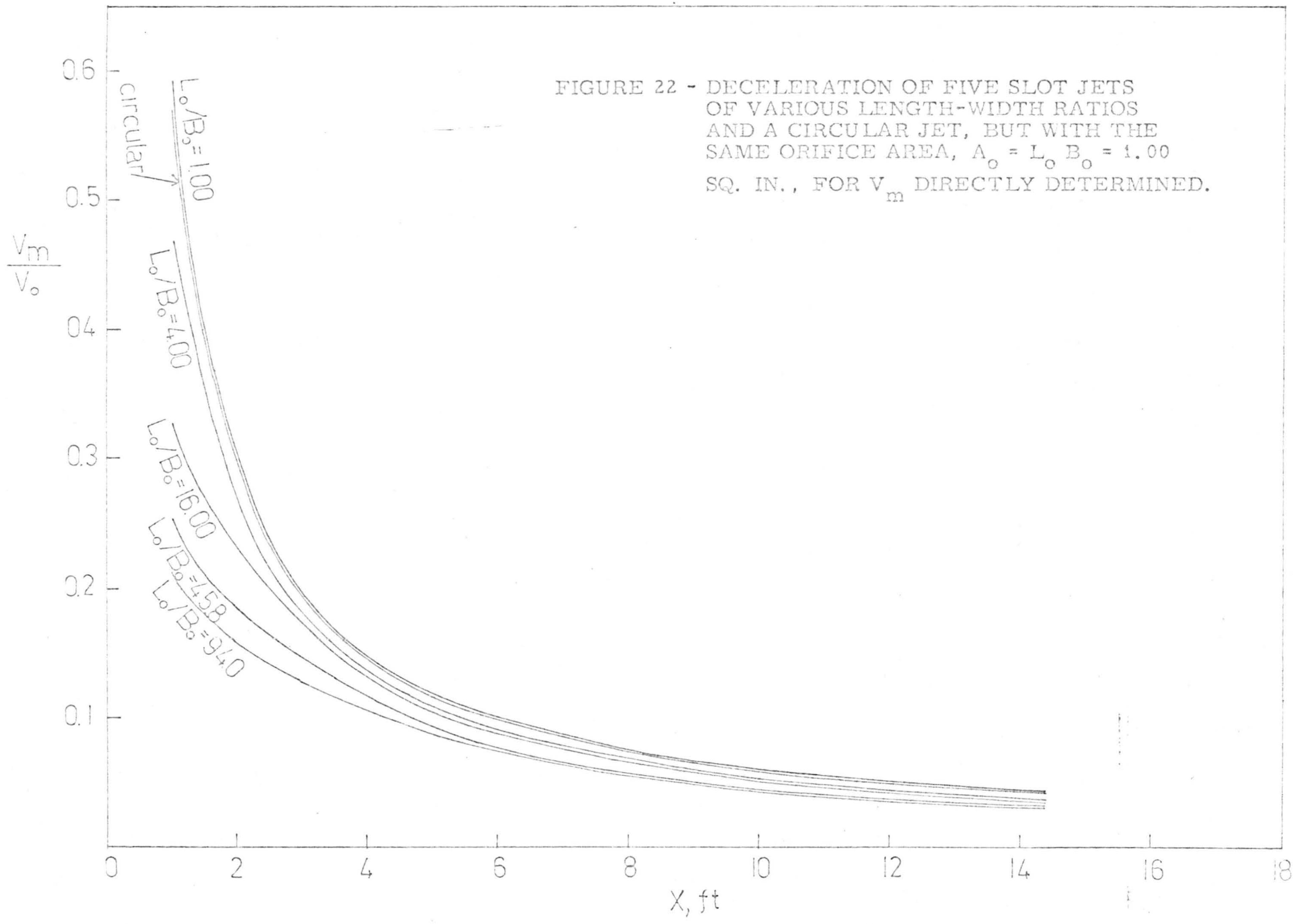

FIGURE 22 - DECELERATION OF FIVE SLOT JETS OF VARIOUS LENGTH-WIDTH RATIOS AND A CIRCULAR JET, BUT WITH THE SAME ORIFICE AREA, $A_o = L_o B_o = 1.00$ SQ. IN., FOR V_m DIRECTLY DETERMINED.

$$\Delta X = X_4 (1.28 v \sqrt{a} - 1) \tag{26}$$

for $X_o \leq X_4 \leq X_2$, or the relative difference $\Delta X/X_4$ becomes a constant for given "v" and "a", within the given range of X_4. This difference, therefore, decreases with a decrease of "v" for a constant "a", but increases with an increase of "a" for a constant "v." For $a = 100$ and $v = 0.1$, this relative difference is 0.28, or 28 percent.

For the region of $X > X_2$, the square jet values of X are the same as above, and equation (25) gives the X value of slot jets for $L_o/B_o = a$ as $X_5 = 7.5 \sqrt{A_o}/(v\, a^{0.065})$. The difference $\Delta X = X_3 - X_5$ becomes

$$\Delta X = X_5 (a^{0.065} - 1) \tag{27}$$

for $X_5 \geq X_2$, or the relative difference $\Delta X/X_5$ becomes a constant for a given "a", and is independent of "v." For $a = 100$, this relative difference is 0.35, or 35 percent. For $a = 10$, it is only 0.16 or 16 percent.

Figures 21 and 22 show that the circular and square jets penetrate deeper into the environmental fluid at rest for a given V_m/V_o ratio, than the slot jets, when the penetration is measured by this ratio. However, as it will be shown later, this greater penetration of jets with geometrically more concentrated orifice cross sections (circular, square, low value L_o/B_o) consequently has a smaller volume entrainment of environmental fluid than the slot jets of greater length-width ratio.

.3.5 Ellipticity of isovels

Isovels are defined here as isolines of equal time-average velocities which are parallel to jet-axis in a cross section perpendicular to the jet-axis. For a two-dimensional jet, the isovels theoretically are parallel, and for a circular jet they are circles. In a slot jet with a finite value L_o/B_o, the isovels are expected to be elliptical after a limited length of jet expansion, where the effects of slot angles have been attenuated or washed out.

Figure 23 shows the isovels of the slot jet having the largest value length-width ratio ($L_o/B_o = 94$) experimented with in this study, for the position three feet above the nozzle. Though the isovels are based only on five recorded traverses, using velocities from the fitted Gaussian curves, they show evidently that slots having very large L_o/B_o ratios have a limited domain of elliptical isovels before the distribution of velocities practically approximates circular isovels. It was noted in some cases that the long elliptic axis, of the original isovel which is parallel to the Z-axis of the slot side L_o, may even change the direction by 90^0 at a greater distance from the orifice, as shown in figure 23. Though the experimental evidence is limited and nonconclusive, some experiments point out that diffusion effects from the ends of the long side of the orifice may be producing an alternation in the direction of ellipticity. However, it seems that an attenuating effect exists in this alternation, with a convergence to the circular isovels. The effect of this change in ellipticity may be caused by the blower type air supply, with the influence of vorticity induced by the blower blades. It is evident that the isovels of slot jets tend to those of circular jets with the progress of jet expansion. This explains the

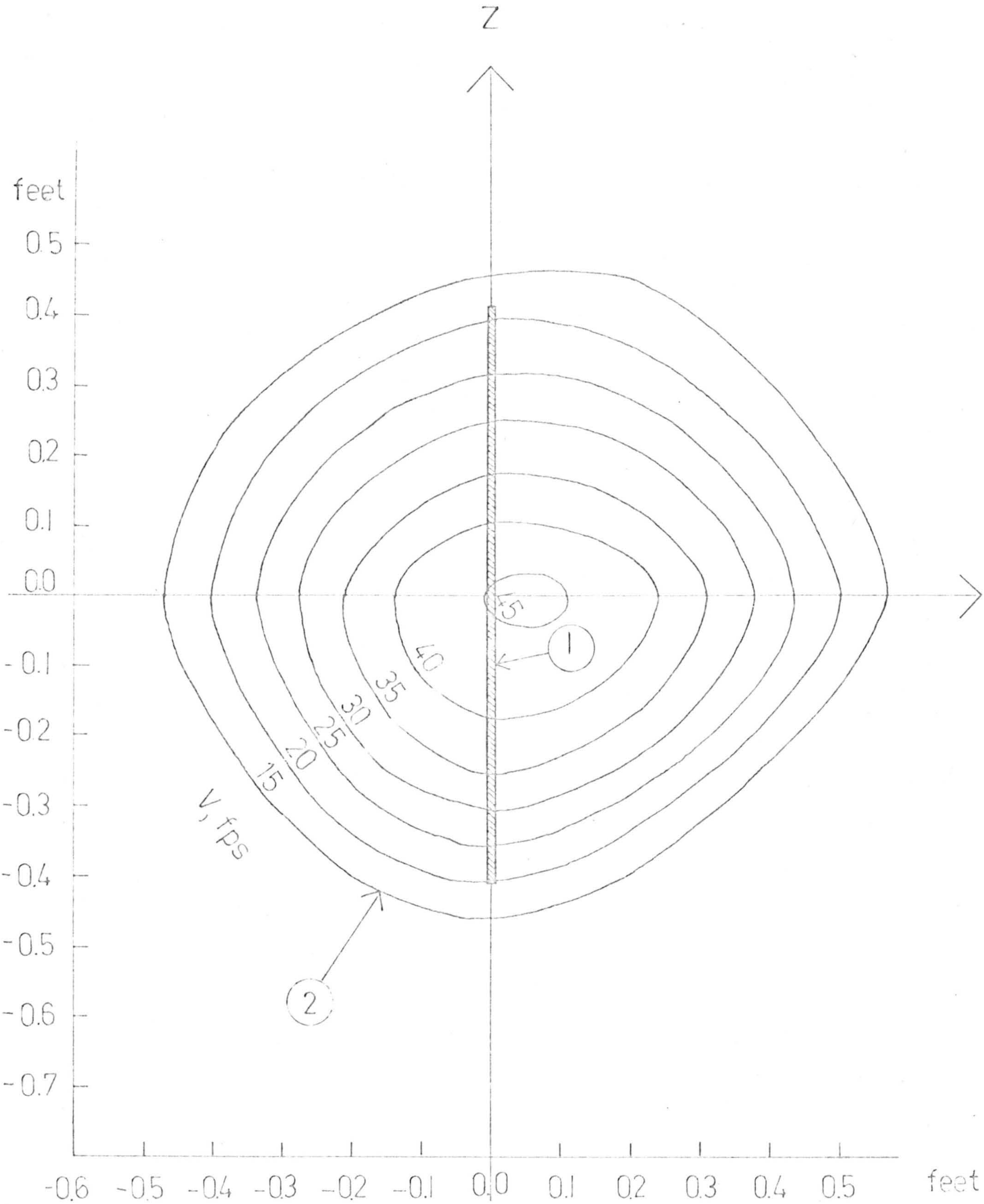

FIGURE 23 - ISOVELS OF THE SLOT JET WITH ORIFICE LENGTH-WIDTH RATIO 94.0 AT THE 3 FEET DISTANCE FROM THE ORIFICE:

(1) Slot orifice position;

(2) Isovels.

fact that the slot jet velocity deceleration follows the slope of the circular jet deceleration line for sufficiently large relative distances, greater than X_2/B_o, which in turn depend on L_o/B_o ratio.

.3.6 Flow rate increase with distance

Figure 24 shows the relationship of Q/Q_o versus X/B_o in log-log scales, for various L_o/B_o ratios with Q the flow rate at any cross section X, and Q_o the flow rate through the orifice nozzle. The perimeter of a slot orifice is $P = 2(L_o + B_o) = 2(a+1)\sqrt{A_o/a}$ with $a = L_o/B_o$ the orifice length-width ratio. An increase of "a" means an increase in perimeter because $(a+1)/\sqrt{a}$ increases with "a"; for $a = 1$, $P = 4\sqrt{A_o}$; for $a = 9$, $P = 6.67\sqrt{A_o}$, and for $a = 100$, $P = 20.2\sqrt{A_o}$. The longer the perimeter of the orifice, the larger is the contact area between the slot jet and the surrounding fluid in the establishing and even at the beginning of established flow zone. Therefore, for the same position X along the jet-axis, the entrained flow rate should increase with an increase of L_o/B_o ratio. A plot of Q/Q_o versus X in cartesian scales (not presented here), shows this fact more clearly than figure 24.

Because the number of traverses at a cross section perpendicular to the jet-axis, X distant from the orifice, was limited to five, the accuracy of flow rate determination was not very great. This resulted in a relatively wide spread of points Q/Q_o versus X/B_o in figure 24. Regardless of this low accuracy, the trend is clear that the slot jets with larger L_o/B_o values having the positions in figure 24, which are all to the right of the sloping line for circular jet, and they are parallel to the slope of circular jet beyond a value X_{2Q}. For values $X < X_{2Q}$, the relationship of Q/Q_o versus X/B_o

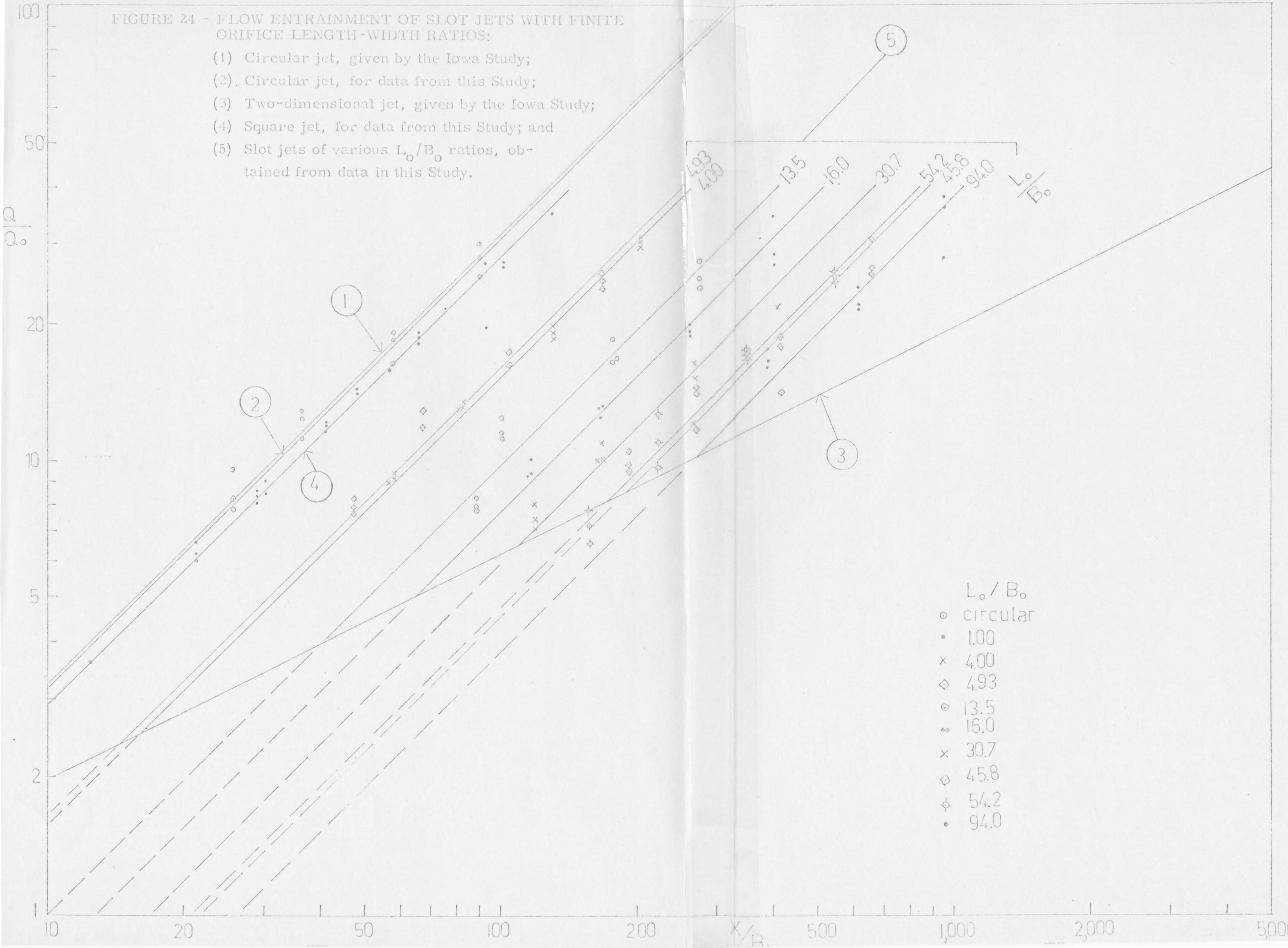

FIGURE 24 - FLOW ENTRAINMENT OF SLOT JETS WITH FINITE ORIFICE LENGTH-WIDTH RATIOS:

(1) Circular jet, given by the Iowa Study;
(2) Circular jet, for data from this Study;
(3) Two-dimensional jet, given by the Iowa Study;
(4) Square jet, for data from this Study; and
(5) Slot jets of various L_o/B_o ratios, obtained from data in this Study.

for two-dimensional jet is valid for slot jets of any L_o/B_o ratio.

Similarly as for the relationship $V_m/V_o = f(X/B_o)$, the values X_{1Q}/B_o as intersections of straight lines (fitted to points in fig. 24 by least squares method) and the horizontal line $Q/Q_o = 1$ are plotted versus L_o/B_o, figure 25. A least squares fit, figure 25, line (1), gives

$$\frac{X_{1Q}}{B_o} = 3.35 \left(\frac{L_o}{B_o} \right)^{0.462} . \tag{28}$$

The intersection of the straight lines parallel to the circular jet line, which pass through X_{1Q}/B_o as given by the above equation (28), and the straight line of two-dimensional jet, as given by equation (16), determine X_{2Q}/B_o values

$$\frac{X_{2Q}}{B_o} = 4.31 \left(\frac{L_o}{B_o} \right)^{0.924} . \tag{29}$$

The relative flow rate Q/Q_o increases, therefore, as follows:

$$\frac{Q}{Q_o} = 0.62 \sqrt{\frac{X}{B_o}} \tag{30}$$

as given by equation (6) of this report for

$$\frac{X}{B_o} \leq \frac{X_{2Q}}{B_o}, \quad \text{and} \quad \frac{X_{2Q}}{B_o} \text{ given by equation (29);}$$

and,

$$\frac{Q}{Q_o} = 0.298 \left(\frac{L_o}{B_o} \right)^{-0.462} \frac{X}{B_o} \tag{31}$$

RELATIVE ENERGY FLUX FOR SLOT JETS OF VARIOUS LENGTH-WIDTH RATIOS:

(1) Straight line fit for flow rate of $\log (X_{1Q}/B_o) = f_Q (\log L_o/B_o)$ by least squares method; and,

(2) Straight line fit of energy flux of $\log (X_{1E}/B_o) = f_E (\log L_o/B_o)$ by least squares method.

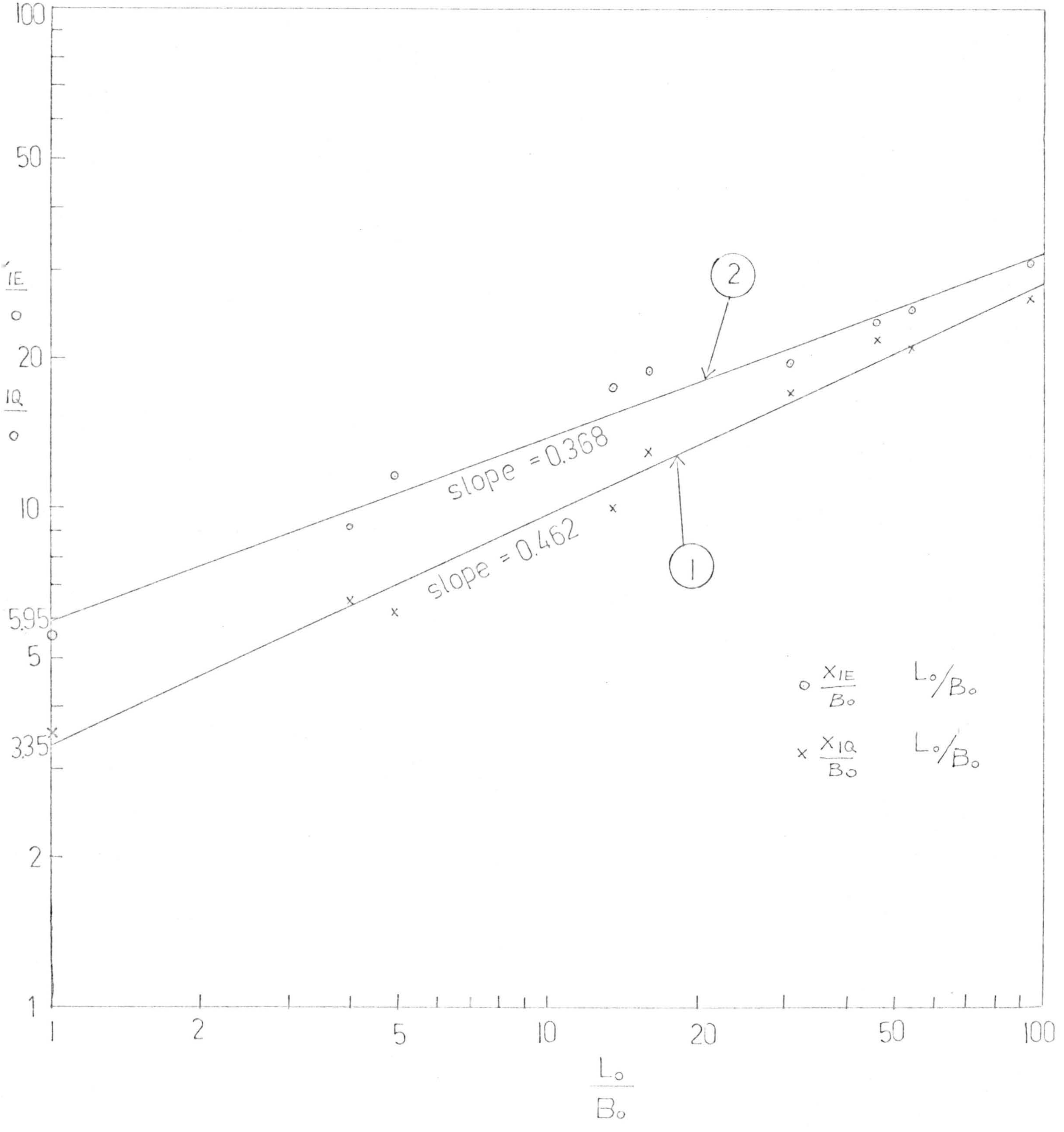

for

$$\frac{X}{B_o} \geq \frac{X_{2Q}}{B_o} .$$

Because of the inaccuracy in determining the distribution of time-average velocities in Y-Z plane by recording the velocity pressures only along five traverses, equations (28) through (31) must be considered only as first approximations. Figure 26 represents the results of equations (30) and (31), as the final approximate results of this study for the change of Q/Q_o with X/B_o.

. 3.7 Energy flux decrease with distance

Figure 27 shows in log-log scales the relationship of relative energy flux E/E_o through a cross section perpendicular to the jet-axis versus the distance X/B_o, with E = energy flux in that section, and E_o energy flux at the orifice. The points E/E_o versus X/B_o have been plotted, and the straight lines parallel to the straight line of the circular jet fitted by least square method for various L_o/B_o ratios. A plot of E/E_o versus X in cartesian scales (not represented here) more clearly demonstrates that the relative energy flux at a given X distance decreases with an increase of L_o/B_o ratio than figure 27.

The same procedures used for V_m/V_o and Q/Q_o gives the following equations for E/E_o by using figure 25, line (2) as the fitted straight line relationship of X_{1E}/B_o versus L_o/B_o,

$$\frac{X_{1E}}{B_o} = 5.95 \left(\frac{L_o}{B_o} \right)^{0.368} \tag{32}$$

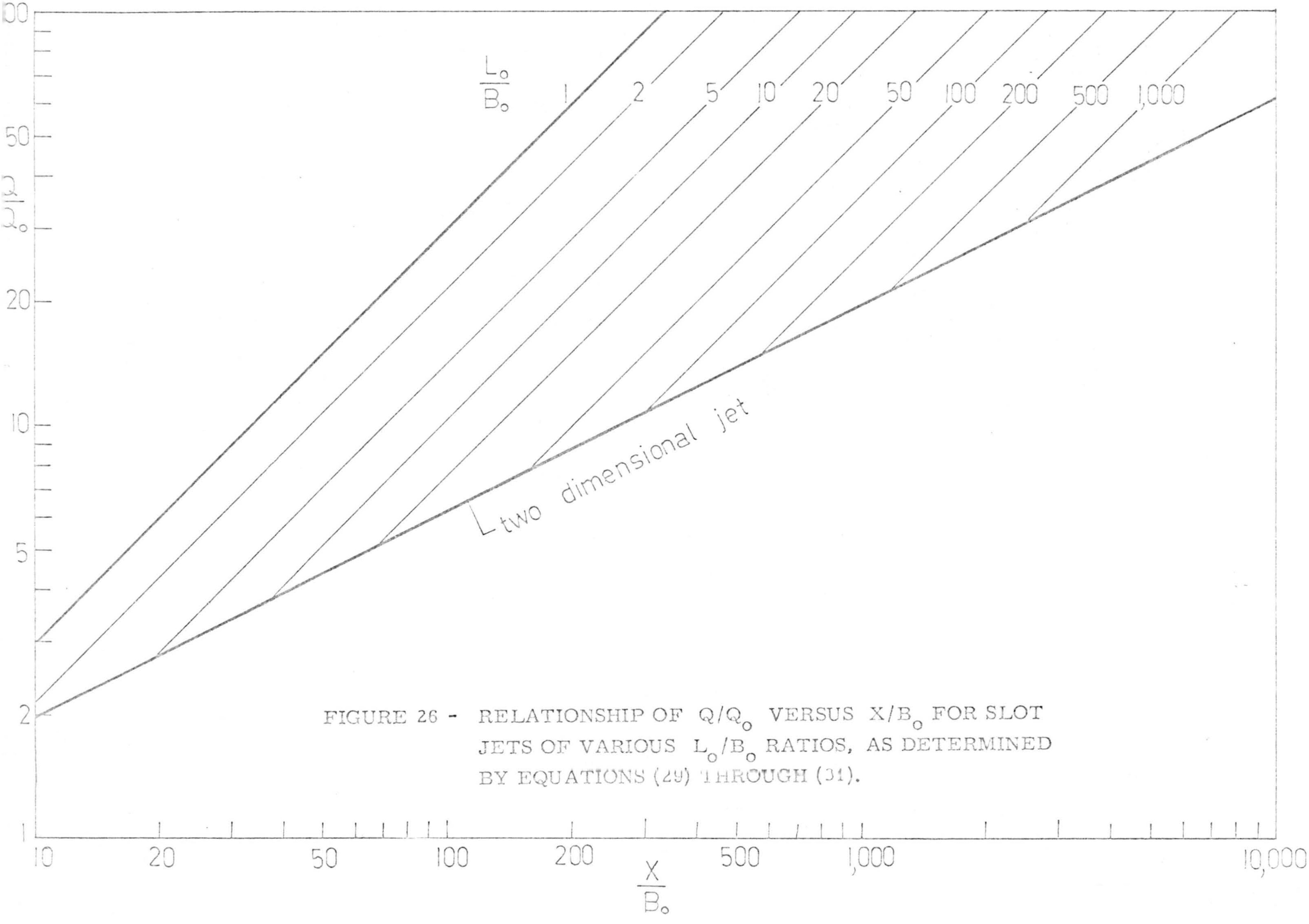

FIGURE 26 - RELATIONSHIP OF Q/Q_o VERSUS X/B_o FOR SLOT JETS OF VARIOUS L_o/B_o RATIOS, AS DETERMINED BY EQUATIONS (29) THROUGH (31).

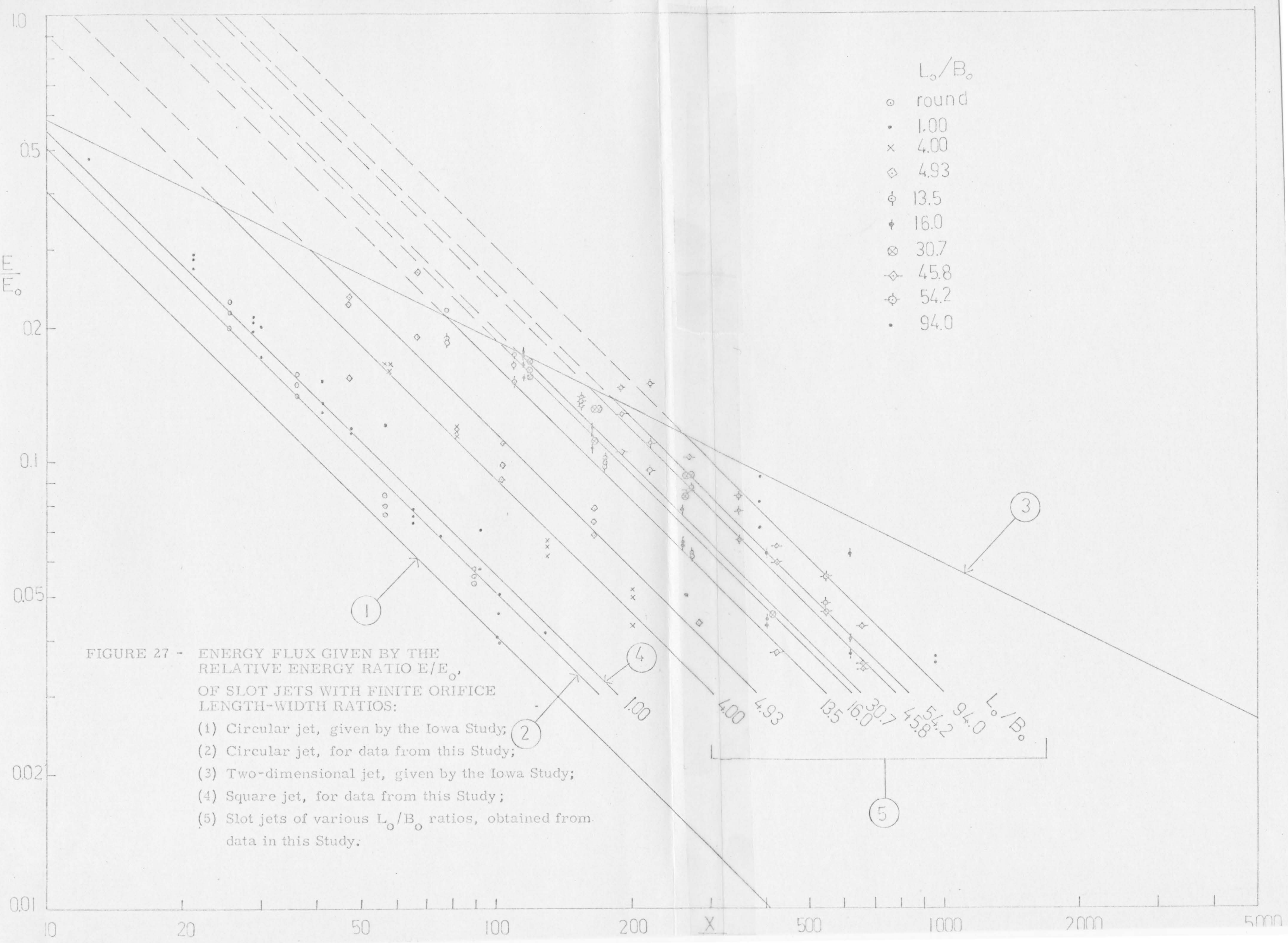

FIGURE 27 - ENERGY FLUX GIVEN BY THE RELATIVE ENERGY RATIO E/E_o, OF SLOT JETS WITH FINITE ORIFICE LENGTH-WIDTH RATIOS:

(1) Circular jet, given by the Iowa Study;
(2) Circular jet, for data from this Study;
(3) Two-dimensional jet, given by the Iowa Study;
(4) Square jet, for data from this Study;
(5) Slot jets of various L_o/B_o ratios, obtained from data in this Study.

and then

$$\frac{X_{2E}}{B_o} = 10.23 \left(\frac{L_o}{B_o} \right)^{0.736} \tag{33}$$

with

$$\frac{E}{E_o} = 1.86 \sqrt{\frac{B_o}{X}} \tag{34}$$

as given by equation (8) of this report, for

$$\frac{X}{B_o} \leq \frac{X_{2E}}{B_o} \text{ ; and , for } X/B_o \geq X_{2E}/B_o.$$

$$\frac{E}{E_o} = 5.95 \left(\frac{L_o}{B_o} \right)^{0.368} \frac{B_o}{X} . \tag{35}$$

These relationships, equations (32), (33) and (35), should be considered only as first approximations because of the errors involved in the Study. Figure 28 represents the results of equations (32) through (35), as the final approximate results of this Study for the change of the E/E_o with X/B_o.

3.8 Standard deviation of time-average distributions in the central traverse.

Figure 29 shows the change of standard deviation of time-average velocity distributions in the central traverses with the distance along the X-axis. This is the central traverse at a given X (see fig. 3). This data, though subjected to several sources of errors, shows that even for the circular jet the ratio σ/X, or the standard deviation over the distance along the jet-axis, is not a constant. All points in the graph, as well as the approximate straight lines drawn through the points for

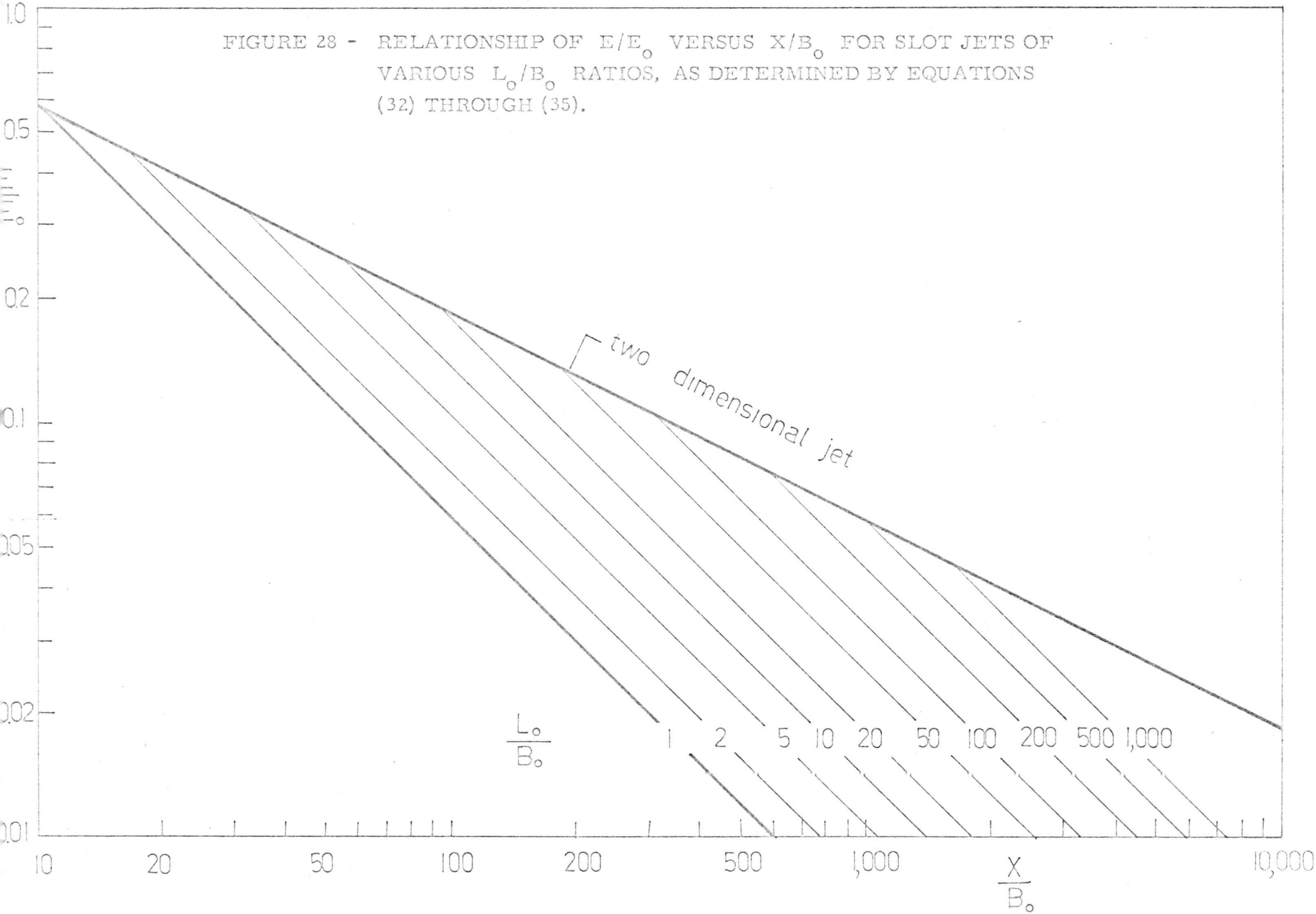
FIGURE 28 - RELATIONSHIP OF E/E_o VERSUS X/B_o FOR SLOT JETS OF VARIOUS L_o/B_o RATIOS, AS DETERMINED BY EQUATIONS (32) THROUGH (35).
two dimensional jet
$\frac{L_o}{B_o}$
1
2
5
10
20
50
100
200
500
1,000
1.0
0.5
0.2
0.1
0.05
0.02
0.01
$\frac{E}{E_o}$
10
20
50
100
200
500
1,000
10,000
$\frac{X}{B_o}$

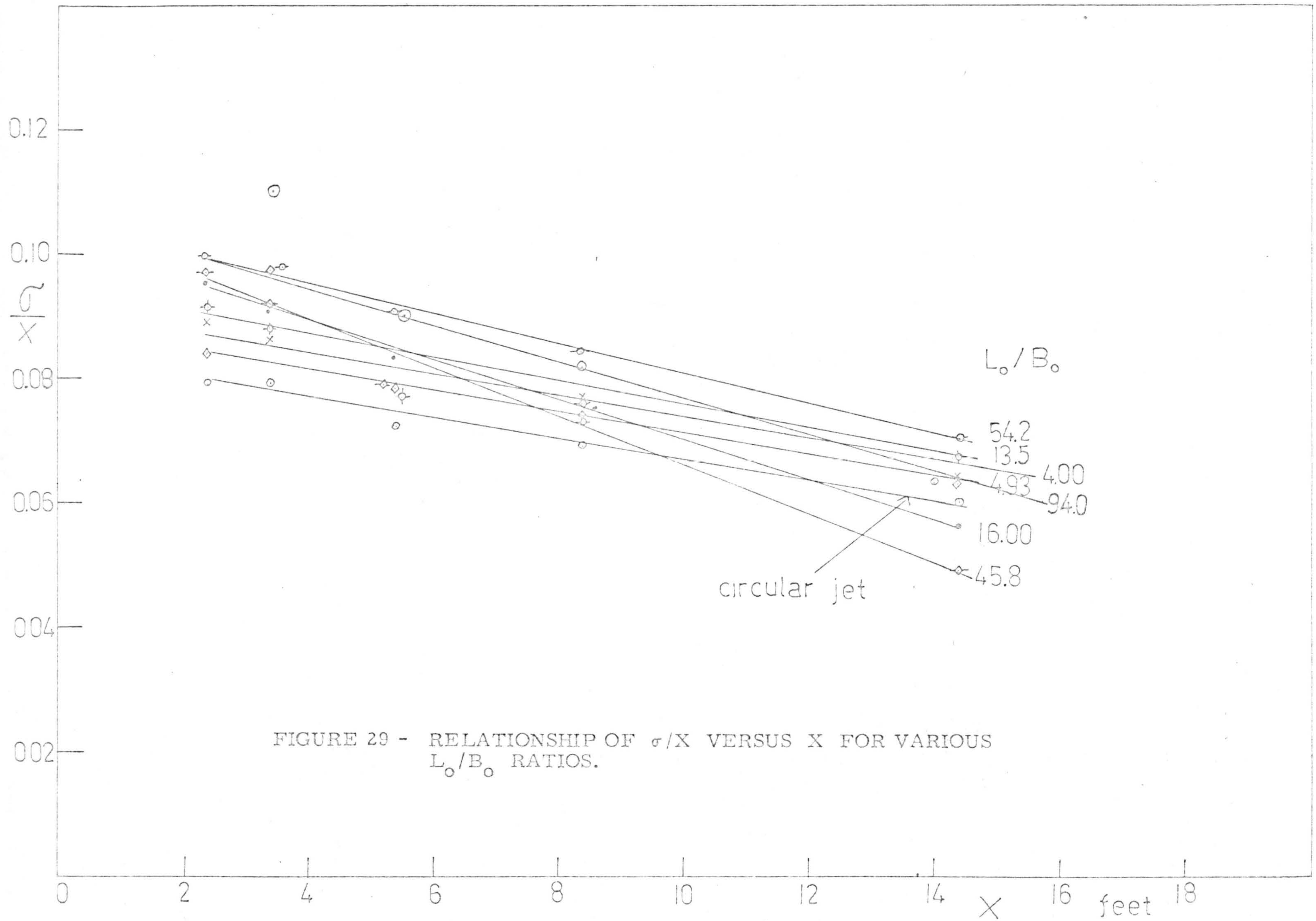

FIGURE 29 - RELATIONSHIP OF σ/X VERSUS X FOR VARIOUS L_o/B_o RATIOS.

some values L_o/B_o, show that σ/X decreases with the distance X. Though this study has not produced a sufficient accuracy of σ for a detailed analysis either of σ/X versus X/B_o or σ/X versus X, it may be expected that σ/X is not constant, and that its change with X/B_o or X warrant further investigation.

REFERENCES

1. Betz, A., 1923 [in German], Versuche ueber die Ausbreitung eines freien Strahles (Experiments on expansion of a free jet): Ergebnisse der Aerodynamischen Versuchsanstalt zu Goettingen II, 1923, pp. 69-73.

2. Tollmien, Walter, 1926 [in German], Berechnung turbulenter Ausbreitungsvorgaenge (Calculation of turbulent expansion processes): Zeitschrift fuer angewandte Mathematik and Mechanik, vol. 6, pp. 468-478. (Translation in English, NASA, TM 1085).

3. Bickley, W., 1929, The plane jets: Phil. Mag., ser. 7, no. 23, 1939, p. 727.

4. Ruden, R., 1933 [in German], Turbulente Ausbreitungsvorgaenge in Freistrahl (Turbulent expansion processes in a free jet): Die Naturwissenchaften, vol. 21, p. 375.

5. Forthmann, E., 1934 [in German], Ueber turbulente Strahlausbrietung (On the turbulent jet expansion): Ingenieur Arch., no. 5, 1934, pp. 42-54.

6. Keuthe, A. M., 1935, Investigations of the turbulent mixing regions formed by jets: Journal of Applied Mechanics, Sept., p. A-87.

7. Taylor, G. I., 1935, Statistical theory of turbulence: Proc. Royal Soc. of London, series A, v. 151, pp. 421-478.

8. Howarth, L., 1938, Concerning the velocity and temperature distribution in plain and axially symmetrical jets: Proceedings, Cambridge Philosophical Society, vol. 34, pp. 185-203.

9. Tomotika, S., 1938, Application of the modified vorticity transport theory to the turbulent spreading of a jet of air: Proceedings, Royal Soc. of London, vol. 165, series A, March-April, p. 65.

10. Towle, W. L., and Sherwood, T. K., 1939, Eddy diffusion-mass transfer in the central portion of a turbulent air stream: Ind. and Eng. Chem., vol. 31, no. 4, April, pp. 457-462.

11. Reichardt, H., 1941 [in German], Ueber eine neue Theorie der freien Turbulenz (On a new theory of free turbulence): Zeitschrift fuer angewandte Mathematik und Mechanik, vol. 21, no. 5, October, pp. 257-264, (Translation in English R. T. P., Trans. no. 1686, British M. A. P.)

12. Goertler, H., 1942 [in German], Berechnung von Aufgaben der freien Turbulenz auf Grund eines neues Naeherungsansatzes (Computation of problems with free turbulence based on a new approximate procedure): Zeitschrift fuer angewandte Mathematik and Mechanik.

13. Reichardt, H., 1942 [in German], Gesetzmaessigkeiten der freien Turbulenz (Regularities in free turbulence): Verein Deutscher Ingenieure, Forschungsheft 414.

14. Corrsin, Stanley, 1943, Investigation of flow in an axially symmetrical heated jet of air: Wartime report W-94, National Advisory Committee for Aeronautics, December 1943, Washington, D. C.

15. Squire, H. B., and Trouncer, F., 1944, Round jets in a general stream: R and M., no. 1974, British A. R. C.

16. Citrini Duilio, 1946 [in Italian], Diffusione di una vena liquida effuente in un campo di fluido in quiete (Diffusion of a liquid current which enters an environment of fluid at rest): L'Energia Elettrica, April 1946.

17. Citrini Duilio, 1946 [in Italian], Ricerca sperimentale sulla diffusione di una vena liquida effluente in un camp di liquido in quiete (Experimental study on the diffusion of a liquid current which enters an environment of liquid at rest): L'Energia Elettrica, August 1946.

18. Maretti, G., 1946 [in Italian], Scie e getti piani turbolenti (Currents and two-dimensional turbulent jets): Rendiconti, Accademia dei Lincei, Rome, Italy.

19. Citrini Duilio, 1947 [in Italian], Nuove ricerche sulla diffusione di una vena liquida in un campo di liquido in quiete (New investigations on the diffusion of a liquid current in an environment of liquid at rest): L'Energia Elettrica, June 1947.

20. Liepmann, H. W., and Laufer, J., 1947, Investigations of free turbulent mixing: Technical Note no. 1257, National Advisory Committee for Aeronautics, Washington, D. C.

21. Baines, W. D., 1948, Investigations in the diffusion of submerged jets: Thesis presented to the State University of Iowa, Iowa City, August 1948.

22. Hinze, J. O., and van der Hegge Zijnen, B. G., 1948, Transfer of heat and matter in the turbulent mixing zone of an axially symmetrical jet: Proc. Seventh International Congress for Applied Mechanics, London, 1948, pp. 286-299.

23. Corrsin, Stanley, and Uberoi, M. S., 1949, Further experiments on the flow and heat transfer in heated turbulent air jet: National Advisory Committee for Aeronautics, Tech. Note no. 1865, April 1949, Washington, D. C.

24. Forstall, Walton, Jr., and Shapiro, Ascher H., 1949, Momentum and mass transfer in coaxial gas jets: Meteor. Rep. No. 39, Dept. Mech. Eng., M. I. T., July (Bur. Ord. Contract NOrd 9661).

25. Hinze, J. O., and Hegge Zijnen, B. G. v. d., 1949, Transfer of heat and matter in the turbulent mixing zone of an axially symmetrical jet: Appl. Scient. Res., section A, no. 1, 1949, pp. 435-461.

26. Keagy, W. R., Weller, A. E., Reed, F. A., and Reid, W. T., 1949, Mixing in inhomogeneous gas jets: Betelle Memorial Inst., The Rand Corp., Santa Monica, Calif., February 1949.

27. Albertson, M. L., Dai, Y. B., Jensen, R. A., and Rouse, Hunter, 1950, Diffusion of submerged jets: Trans. Amer. Soc. Civ. Eng., vol. 115, 1950, pp. 639-697, with discussions.

28. Corrsin, Stanley, and Uberoi, Mahinder S., 1950, Further experiments of the flow and heat transfer in a heated turbulent air jet: National Advisory Committee for Aeronautics, Rep. 998.

29. Grimmett, Howard L., 1950, Entrainment of air jets: Ph. D. thesis, University of Illinois.

30. Squire, H. B., 1950, Jet flow and its effects on aircraft: Aircraft Eng., vol. XXII, no. 253, March, pp. 62-67.

31. Baron, Thomas, and Alexander, L. G., 1951, Momentum, mass, and heat transfer in free jets: Chem. Eng. Prog., vol. 47, no. 4, April, pp. 181-185.

32. Corrsin, Stanley, and Uberoi, M. S., 1951, Spectra and diffusion in a round turbulent jet: National Advisory Committee for Aeronautics, Rept. 1040, 1951, Washington, D. C.

33. Sato, S., and Hosoi, M., 1951 [in Japanese], A study of submerged jet: Technical report of the Research Bureau of Civil Engineering Construction Ministry of Japan, no. 81, pp. 1-13, March 1951.

34. Taylor, J. F., Grimmett, H. L., and Comings, E. W., 1951, Isothermal free jets of air mixing with air: Chem. Eng. Progress, vol. 47, no. 4, April, pp. 175-180.

35. Baron, T., and Bollinger, E. H., 1952, Mixing of high-velocity air jets: Tech. Rep. No. CML-3, Eng. Exp. Station, University of Illinois, March.

36. Alexander, Lloyd G., Baron, Thomas, and Comings, Edward W., 1953, Transport of momentum, mass, and heat in turbulent jets: Bull. ser. no. 413, University of Illinois.

37. Hom-ma, Masashi, 1953, An experimental study on water fall: Proc. IAHR Minnesota International Hydraulics Convention, Sept., 1953, pp. 477-481.

38. Forstall, W., and Gaylord, E. W., 1955, Momentum and mass transfer in a submerged water jet: Journal of Applied Mechanics, v. 22, no. 2, June 1955, pp. 161-164.

39. Squire, H. B., 1955, Radial jets: Paper in "50 Jahre Grenzschictsforschung" (50 years of boundary layer investigation): Edited by Görtler and Tollmien, F. Vieweg and Sons, 1955.

40. Miller, D. R., and Comings, E. W., 1957, Static pressure distribution in the free turbulent jet: Journal of Fluid Mechanics, no. 3, 1957, part I, pp. 1-16.

41. Schmidt, F. H., 1957, On the diffusion of heated jets: Tellus, v. 9, no. 3, August 1957, part I, pp. 378-383.

42. Hegge Zijnen, B. G. v. d., 1958, Measurements of the velocity distribution in a plane turbulent jet of air: Appl. Scient. Res., section A, no. 7, 1958, pp. 256-276.

43. Hegge Zijnen, B. G. v. d., 1958, Measurements of the distribution of heat and matter in a plane turbulent jet of air: Appl. Scient. Res., section A, no. 7, 1958, pp. 177-292.

44. Hegge Zijnen, B. G. v. d., 1958, Measurements of turbulence in a plane jet of air by the diffusion method and by the hotwire method: Appl. Scient. Res., section A, no. 7, 1958, pp. 293-313.

45. Abraham, G., 1959, Diffusion in submerged circular vertical turbulent water jets with density difference between jet and surrounding water: IER, Tech. Rept. 138-2, Hydraulic Eng. Lab., Wave Research Projects, University of California, Berkeley, August 1959.

46. Hart, W. E., 1960, Jet discharge into a fluid with a density gradient: Univ. of Calif., Inst. of Eng. Res., Tech. Rept., series 138, issue 4, November 1960.

47. Abraham, G., 1961, Jet diffusion in liquid of greater density: Am. Soc. of Civil Eng. Trans., v. 126, part I, paper 3095, pp. 76-87 (See also Proc. Am. Soc. of Civil Eng., v. 86, 1960, no. HY6, June, pp. 1-13).

48. Bosanquet, C. H., Horn, G., and Thring, M. W., 1961, The effect of density differences on the path of jets: Proc. Roy. Soc. London, A263, 1961, no. 1314, pp. 340-352.

49. Hart, W. E., 1961, Jet discharge into a fluid with a density gradient: Proc. Am. Soc. Civil Eng., v. 87, no. HY6, 1961, part I, pp. 171-200.

50. Polyakov, E. I., 1961 [in Russian], Soviet Phys. - Tech. Phys. (English Translation), 5, 1173, 1961.

51. Ricou, F. P., and Spalding, D. B., 1961, Measurements of entrainment by axisymmetrical turbulent jets: Journ. of Fluid Mechanics, no. 11, 1961, part I, pp. 21-32.

52. Abraham, G., 1962, Jet dischrage into a fluid with a density gradient: Discussion of paper by Hart, W. E., in Proc. Amer. Soc. of Civil Eng., v. 88, 1962, no. HY2, part 1, March, pp. 195-198.

53. Abraham, G., 1963, Jet diffusion in stagnant ambient fluid: Delft Hydraulics Laboratory, series 1, Fluid Mechanics, Publ. no. 29, July 1963.

54. Craya, A., 1963 [in French], Études récentes sur le comportement des jets (Recent studies of behavior of jets): Journal Génie Chimique, France, vol. 89, no. 2, pp. 33-43 and vol. 89, no. 3, pp. 77-87.

55. Heskestad, Gunnar., 1963, The turbulent shear flows: Report of Department of Mechanics, The John Hopkins University, June 1963, Baltimore, Maryland.

56. Rosler, R. S., and Bankoff, S. G., 1963, Large-scale turbulence characteristics of a submerged water jet: A. I. Ch. E. Journal, v. 9, no. 5, September 1963, pp. 672-676.